

## Article

# System Economy Improvement and Risk Shortening by Fuel Cell-UPFC Placement in a Wind-Combined System

Mitul Ranjan Chakraborty<sup>1</sup>, Subhojit Dawn<sup>2,\*</sup> , Pradip Kumar Saha<sup>3</sup>, Jayanta Bhusan Basu<sup>1</sup>   
and Taha Selim Ustun<sup>4,\*</sup> 

<sup>1</sup> Department of Electrical Engineering, Siliguri Institute of Technology, Siliguri 734009, West Bengal, India

<sup>2</sup> Department of Electrical & Electronics Engineering, Velagapudi Ramakrishna Siddhartha Engineering College, Vijayawada 520007, Andhra Pradesh, India

<sup>3</sup> Department of Electrical Engineering, Jalpaiguri Government Engineering College, Jalpaiguri 735102, West Bengal, India

<sup>4</sup> Fukushima Renewable Energy Institute, AIST (FREA), Koriyama 963-0298, Japan

\* Correspondence: subhojit.dawn@gmail.com (S.D.); selim.ustun@aist.go.jp (T.S.U.)

**Abstract:** It is important to understand the features of an integrated renewable energy power system, especially for deregulated systems. The greatest obstacle to assimilating renewable energy generators with the existing electrical system is their unpredictability. Because wind energy is inconsistent, incorporating it into an established power system necessitates more planning. The effects of wind farm (WF) incorporation with fuel cells and a unified power flow controller (UPFC) on electric losses, voltage profile, generating price, and the economics of the system in a deregulated power market are examined in this paper. An impact analysis of integrating wind farms into controlled and uncontrolled situations is conducted. At two randomly selected locations in India, the real-time statistics of the actual wind speed (AWS) and forecasted wind speed (FWS) were merged for this study. The surplus charge rate and deficit charge rate are intended to evaluate the imbalance cost which is arising from the difference between anticipated and true wind speeds to determine the economics of the system. Customers are always trying to find electricity that is reliable, inexpensive, and efficient due to the reconfiguration of the power system. As a consequence, the security limitations of the system may be surpassed or might function beyond the safety limit, which is undesirable. In the last section, heuristic algorithms, such as sequential quadratic programming (SQP), artificial bee colony algorithms (ABC), and moth-flame optimization algorithms (MFO), are employed to analyze economic risk. In the real-time energy market, it also covers how the fuel cells and UPFC are utilized to rectify the WF integration's deviation. Economic risk evaluation approaches include value-at-risk (VaR) and conditional value-at-risk (CVaR). A modified IEEE 30-bus test system is used throughout the whole project.

**Keywords:** electricity market; wind energy; UPFC; fuel cell; system profit; VaR; CVaR



**Citation:** Chakraborty, M.R.; Dawn, S.; Saha, P.K.; Basu, J.B.; Ustun, T.S. System Economy Improvement and Risk Shortening by Fuel Cell-UPFC Placement in a Wind-Combined System. *Energies* **2023**, *16*, 1621. <https://doi.org/10.3390/en16041621>

Academic Editors: Chuanbo Xu, Jianli Zhou, Shenbo Yang and Liwei Ju

Received: 17 January 2023

Revised: 2 February 2023

Accepted: 4 February 2023

Published: 6 February 2023



**Copyright:** © 2023 by the authors. Licensee MDPI, Basel, Switzerland. This article is an open access article distributed under the terms and conditions of the Creative Commons Attribution (CC BY) license (<https://creativecommons.org/licenses/by/4.0/>).

## 1. Introduction

The capacity to harness and utilize various sources of energy has revolutionized living conditions for people around the world since the beginning of the industrial period. Particularly, the high dependency on fossil fuels poses a major danger to the sustainability of both important human and natural systems by drastically altering the temperature of the planet [1]. Due to the introduction of new technologies that increase consumer comfort and require a lot of electrical power to function, energy demand is rising quickly nowadays. The reform of the electrical system has created intense competition among all the participants in the energy market, including retailers, transmission companies, distribution firms, and generation companies (GENCOs). It fosters an environment where clients can gain additional financial advantages [2].

However, it is exceedingly challenging to build new power stations quickly because of environmental, political, and economic hurdles. Because power supply lags behind power generation, there are several hazards associated with a competitive energy marketplace, including grid failure, severe bottleneck, financial loss to market players, etc. By optimizing the flow of electrical power, the use of renewable energy along with energy storage technologies as a power source provides a method to reduce the gap between power generation and demand.

Due to its affordability, environmental friendliness, accessibility, and independence, wind energy is among the popular renewable energy sources worldwide [3]. Electric utilities must augment their methods for maximizing the flow of power through current transmission networks due to prohibitions on the installation of new transmission lines. The most adaptable and practical alternative for regulating the flow of electricity across transmission lines is thought to be the FACTS devices. In both normal and fault scenarios, it also gives the system voltage stability [4].

Recent research has shown how fuel cells can significantly contribute to backup supply to lower system costs, have a smaller negative impact on the environment, and be less reliant on fossil fuels, while maintaining essential services. The paper [5] by Ma Zhiwen identifies methods for using fuel cells in a large network of fuel cells as distributed energy sources through nano/microgrids.

Thermal units are allowed to participate in electricity markets on most provincial power markets, and renewables are set up with independent system operators (ISO) for electricity generation priority. A two-level model of planned market allocations for electricity is proposed in this study, which considers the generation company's bid-matching games to achieve smooth power system reform transitions [6].

A generation company's (GenCo) profits are maximized by the profit maximization of GenCo's shares in the electric market. Both the demand and supply sides submit bids in a regulated electricity market, and the price forecast is the benchmark for both. Bilateral agreements and energy derivatives use the long-term price estimates of electricity supply as a benchmark [7]. Conejo et al. [8] adopted the price forecast errors to account for pricing uncertainty.

A comprehensive literature review was carried out regarding deregulated electricity systems integrating renewable sources with the help of FACTS devices [9]. Ramesh et al. [10] investigated the efficiency of deregulated power systems incorporated with different energy storage techniques [10]. It is widely recognized that FACTS have a substantial influence on power transmission efficiency. The optimum placement of the distributed power flow controllers (DPFC) within a power grid should take into account operational costs and the investment of installed DPFCs [11]. Voltage and frequency fluctuations in island electrical systems are caused by fluctuations in electricity supply from renewable sources. When the power grid is shut down, the distributed generation still provides the needed electricity for that segment of the local loads [12].

Scientists published a study in *Energy & Environmental Science* on how to extend the life of solid oxide fuel cells, which are used to generate hydrogen and electricity [13]. In a WF-integrated power system, to reduce the system risk as well as to reduce system-generated costs, the storage systems are placed optimally within the electricity grid, applying the artificial honeybee colony (ABC) and moth-flame optimization (MFO) algorithms [14]. To address energy dispatch problems, hybrid algorithms using enhanced differential evolution (EDE) and a genetic algorithm (GA) were applied by the authors of [15]. Nature-inspired optimization algorithms include stability of frequency [16,17], cost optimization [18], energy management [19], and optimization of storage [20,21].

Although, in earlier times, various placement strategies and associated problems for WPGs, FACTS, or fuel cells, either independently or partially combining them, have been examined, no one, to the best knowledge of the authors, has tackled all these concerns concurrently. To answer these questions, which have not previously been addressed, we took all of the aforementioned factors into account.

The analysis of the literature survey indicates that studies have been conducted on various features of a deregulated system in conjunction with wind generation and energy storage systems. There were few areas to explore in this region, though the following questions were proposed: (a) From an economic and methodological perspective, what are the effects of incorporating wind power to the regulated as well as uncontrolled energy networks? (b) What relationship does the energy market's system revenue have with imbalance costs? (c) How is the system's profitability impacted by the disagreement between anticipated and real wind speeds? (d) In a deregulated electricity market, how does demand-side bargaining affects prices?

The present study examines all of the difficulties and places a strong emphasis on providing answers to all of these queries. The main features of this research include the following:

- This work analyzes and distinguishes regulated systems and deregulated systems where wind power is present in the system;
- A methodology is designed to investigate the implications on the power system due to the unpredictability of the wind speed with integrated wind power in a deregulated electricity scenario. If the actual and expected wind speeds diverge after the GENCOs and DISCOs form a power supply contract based on a wind speed estimate, the ISO may impose a penalty or reward the GENCOs for the excess or shortfall in power delivery. Hence, to mitigate the adverse impact of cost imbalances, GENCOs are making efforts to reduce the power gap between actual and forecast wind speeds;
- The best solution to address this shortage of power is an energy storage system. In a global energy market, storage technology systems can reduce power differences and the load on thermal power plants, allowing the financial return to be realized;
- Depending on the projected and actual wind speed for a whole day, the effect of the imbalance cost of the system on profit is discussed for two distinct sites in India;
- In this case, a fuel cell is used to deal with the adverse impact of cost imbalances in the thermal–wind–fuel cell combined system;
- To assess the efficiency of the recommended technique, SQP, ABC, and MFO are employed;
- Different optimization approaches are used here to highlight the proportional analyses of system risk before and after the deployment of fuel cells;
- The imbalance cost's impact is evaluated. The uniqueness of this research lies in the utilization of a fuel cell to optimize profit, while reducing the impact of cost imbalances, since it has never been conducted before;
- This analysis also establishes how the location of the fuel cells and the UPFC affects the system risk profile.

## 2. Mathematical Modeling

Here, considering the speed of wind at specific elevations, the generated wind power, and the cost of the wind power investment formulation, we examine the costs associated with an imbalance in a deregulated energy system.

### 2.1. Wind Speed Data

To begin with, two places in India (Delhi and Mumbai) were chosen to confirm the results using the data on wind speeds that have been collected. Real-time data on the actual and predicted wind speeds for the selected areas were collected at an elevation of 10 m [22,23]. To do an analysis, it is essential to determine the potential wind speed at that particular height (in India, the wind turbine hub height is 120 m). The investigation into the efficacy of the suggested strategy used the actual and predicted wind speeds, which are shown in Table 1.

According to the specifications, the equation of power law [24] was applied to determine the wind speed at a specified height:

$$\frac{WS_h}{WS_r} = \left(\frac{h}{10}\right)^N \quad (1)$$

where 'WS<sub>h</sub>' = wind velocity at height 'h', 'WS<sub>r</sub>' = reference wind velocity at a height of 10 m, and 'N' = Hellman's coefficient. h was chosen as 120 m.

**Table 1.** FWS and AWS at 10 m elevation (in m/s).

| Hour of the Day | Wind Speed of Mumbai |        | Wind Speed of Delhi |        |
|-----------------|----------------------|--------|---------------------|--------|
|                 | Forecasted           | Actual | Forecasted          | Actual |
| 1.              | 2.22                 | 2.22   | 2.22                | 2.22   |
| 2.              | 2.22                 | 2.50   | 1.67                | 2.22   |
| 3.              | 2.22                 | 1.94   | 1.67                | 2.22   |
| 4.              | 2.22                 | 2.22   | 1.67                | 2.22   |
| 5.              | 2.22                 | 2.22   | 1.94                | 2.22   |
| 6.              | 2.22                 | 1.94   | 1.94                | 2.22   |
| 7.              | 2.22                 | 1.94   | 1.67                | 2.22   |
| 8.              | 2.50                 | 2.22   | 1.94                | 2.22   |
| 9.              | 2.78                 | 2.50   | 1.94                | 2.50   |
| 10.             | 3.06                 | 2.50   | 1.67                | 2.50   |
| 11.             | 3.06                 | 3.06   | 1.67                | 2.22   |
| 12.             | 3.06                 | 3.61   | 1.67                | 2.22   |
| 13.             | 3.61                 | 3.89   | 2.22                | 2.50   |
| 14.             | 3.89                 | 4.17   | 2.50                | 2.50   |
| 15.             | 4.17                 | 4.44   | 2.50                | 2.50   |
| 16.             | 4.44                 | 4.44   | 2.50                | 2.50   |
| 17.             | 4.72                 | 4.17   | 2.22                | 2.22   |
| 18.             | 4.44                 | 3.33   | 1.94                | 1.94   |
| 19.             | 3.89                 | 2.78   | 1.94                | 1.94   |
| 20.             | 3.33                 | 2.50   | 1.94                | 1.94   |
| 21.             | 2.78                 | 2.50   | 1.94                | 1.94   |
| 22.             | 2.50                 | 2.22   | 2.22                | 1.94   |
| 23.             | 2.22                 | 1.94   | 2.22                | 1.94   |
| 24.             | 1.94                 | 1.94   | 2.22                | 2.22   |

## 2.2. Wind Power and Cost Estimation

The main factors that affect wind energy production are air density, wind speed, swept area, and the efficiency of the turbine. The wind power (WP) generated can be reflected as:

$$P_w = \frac{1}{2} D_{air} A_t \eta WS_h^3 \quad (2)$$

where 'D<sub>air</sub>' = the air density (in kg/m<sup>3</sup>), 'A<sub>t</sub>' = turbine's swept area in (m<sup>2</sup>), and η = the overall efficiency of the wind plant. In our work we have taken D<sub>air</sub> = 1.225 kg/m<sup>3</sup>, η = 0.49, and the radius of the turbine rotor (r) = 40 m.

According to the wind speed data, as mentioned in Table 1, the average wind speed for all the designated sites is between 1.67 m/s and 4.72 m/s. The wind power generation costs are \$3.75/MWh to invest [25]. It is anticipated that the power facility would concurrently install 50 turbines. Table 2 summarizes the speed of the wind at the necessary height, the amount of energy that can be generated from the wind, and the wind cost associated with various wind speeds.

**Table 2.** Wind speed and the corresponding investment costs for wind power.

| Sl. No. | Wind Velocity at 10 m (m/s) | Wind Velocity at 120 m (m/s) | Wind Power with 50 Turbines (MW) | Wind Gen Cost with 50 Turbines (\$/h) | Sl. No. | Wind Speed at 10 m (m/s) | Wind Speed at 120 m (m/s) | Wind Power with 50 Turbines (MW) | Wind Gen Cost with 50 Turbines (\$/h) |
|---------|-----------------------------|------------------------------|----------------------------------|---------------------------------------|---------|--------------------------|---------------------------|----------------------------------|---------------------------------------|
| 1       | 1.67                        | 2.38                         | 1.01                             | 3.799                                 | 7       | 3.33                     | 4.75                      | 8.10                             | 30.389                                |
| 2       | 1.94                        | 2.77                         | 1.61                             | 6.032                                 | 8       | 3.61                     | 5.15                      | 10.30                            | 38.637                                |
| 3       | 2.22                        | 3.17                         | 2.40                             | 9.004                                 | 9       | 3.89                     | 5.55                      | 12.87                            | 48.257                                |
| 4       | 2.50                        | 3.57                         | 3.42                             | 12.820                                | 10      | 4.17                     | 5.94                      | 15.83                            | 59.353                                |
| 5       | 2.78                        | 3.96                         | 4.69                             | 17.586                                | 11      | 4.44                     | 6.34                      | 19.21                            | 72.033                                |
| 6       | 3.06                        | 4.36                         | 6.24                             | 23.407                                | 12      | 4.72                     | 6.73                      | 23.04                            | 86.401                                |

To increase economic profits by combining wind power stations with UPFCs in a competitive double-auction power market, a UPFC static model has been employed in this study.

### 2.3. UPFC Static Model

A UPFC is the FACTS component with the widest range of applications for controlling voltage and power flow in transmission lines. It may alter the series injected voltage's amplitude and phase angle simultaneously or individually, as well as the reactive current drawn by the shunt-coupled voltage source converter. By adjusting the transmission line's series reactance together with shunt-connected reactive power injections or extractions on the associated bus, the UPFC may be used as either a capacitive or an inductive compensation, respectively. Here, a DC link connects two voltage source converters that are coupled together to form a UPFC. Figure 1 depicts the transmission line architecture with the UPFC static model where a specific UPFC is linked between buses  $i$  and  $j$ .

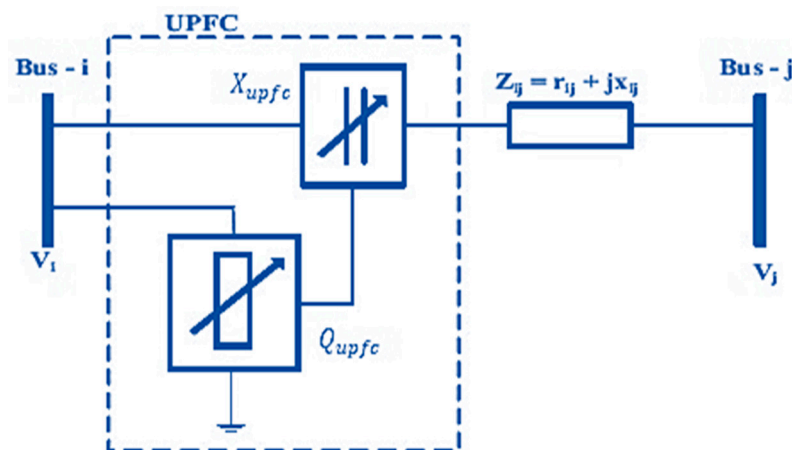


**Figure 1.** UPFC static modeling.

The UPFC's reactance is influenced by the reactance of the transmission line where it will be placed:

$$X_L = X_{i-j} + X_{upfc} \quad (3)$$

where

$$X_{upfc} = \text{UPFC's series converter's reactance} = X_L \times k_{upfc} \quad (4)$$

$X_L$  = total line reactance between bus  $i$  and  $j$  (at the location of the UPFC).

The UPFC compensation level's range is considered as [26,27]  $-0.7 \leq k_{upfc} \leq 0.2$ . Because 100% compensation will cause a resonance issue in the series circuit of the system, the safe limit of the reactance of the line is considered as 70% for compensation. According to the model, as it is presented, the  $Q_{upfc}$  delivers or drains reactive power through a shunt converter at the line's designated bus, which is where the UPFC is situated.

#### 2.4. Investment Cost of the UPFC

Due to the substantial capital costs of UPFC devices, a cost optimization approach for their deployment is crucial. The employed UPFC investment cost models were inspired by [28–35]. In this study, the UPFC device's lifespan (LS) and rate of interest ( $I_r$ ) are considered to be 0.05 and 15 years, respectively. The following formula has been utilized to calculate the UPFC's investment cost:

$$IC_{upfc} = 0.0003S_{oz}^2 - 0.2691S_{oz} + 188.22 \text{ \$/kVar} \quad (5)$$

where

$$S_{oz} = \text{operating zone or range of UPFC} = |Q_x| - |Q_y| \text{ MVar} \quad (6)$$

$Q_x$  = flow of reactive power in the line post-UPFC installation, and  $Q_y$  = flow of reactive power in the line before UPFC installation.

The total investment cost for UPFC devices is computed as:

$$T\_IC_{upfc} = (IC_{upfc} \times S_{oz} \times 1000) \text{ \$} \quad (7)$$

Due to UPFC devices' high cost, a cost assessment is required to find out if a new UPFC device is the most cost-effective option among potential installation locations. In this regard, the investment cost is transformed into a per-year value using the following equation:

$$AT\_IC_{upfc} = T\_IC_{upfc} \frac{I_r(1 + I_r)^{LS}}{(1 + I_r)^{LS} - 1} \text{ \$} \quad (8)$$

where  $AT\_IC_{upfc}$  = annual UPFC investment cost considering all the factors mentioned above.

#### 2.5. Fuel Cell Model

An electrolyzer employs the reverse reaction to electrolyze water to produce hydrogen; while using hydrogen as fuel, a fuel cell turns the chemical energy into electrical energy. Together, these components make up the storage system. The following equation shows the reversible chemical interaction between oxygen and hydrogen, which results in the production of electrical energy, heat, and water.



In tanks, the generated hydrogen is kept, enabling the utilization of the gas for both short- and long-term storage. In comparison to large-scale storage systems such as batteries or pumped hydro storage, the efficiency of hydrogen storage is quite high [36]. The storage system operates according to the following principle:

### 2.5.1. Low-Demand Period (The Electrolyzer Produces Hydrogen to Be Stored in Tanks)

The consumed energy by the electrolyzer is represented as:

$$E_{\text{elz}} = \frac{h\nu_{\text{H}_2}^1 \times E_{\text{H}_2}^{\text{P}}}{\eta_{\text{elz}}} \quad (10)$$

where  $E_{\text{H}_2}^{\text{P}}$  = hydrogen produced by the electrolyzer;

$E_{\text{elz}}$  = energy consumed by the electrolyzer;

$\eta_{\text{elz}}$  = efficiency of the electrolyzer;

$h\nu_{\text{H}_2}^1$  = lower heating value of hydrogen.

### 2.5.2. High-Demand Period (Stored Hydrogen to Be Used in the Fuel Cell to Supply the Demand)

The fuel cell produces electricity using hydrogen during peak hours, and the power-producing capacity is directly related to the use of hydrogen.

$$E_{\text{fc}} = \eta_{\text{fc}} \times \text{fc}_{\text{H}_2}^{\text{con}} \times h\nu_{\text{H}_2}^1 \quad (11)$$

where

$E_{\text{fc}}$  = energy produced from the fuel cell;

$\text{fc}_{\text{H}_2}^{\text{con}}$  = hydrogen consumption in the fuel cell;

$\eta_{\text{fc}}$  = efficiency of the fuel cell.

### 2.6. Social Welfare (SW) and Locational Marginal Pricing (LMP)

The mismatch between society's acceptance of paying for its need for energy and the expense of providing that demand is known as social welfare. The cost and supply of power for a certain provider 'i' is expressed as [37]:

$$P_i = \text{RP}_i + m_G P_{G(i)} \quad (12)$$

where  $P_i$  = the cost that 'i' is ready to provide (\$/MWh);

$\text{RP}_i$  = the intercept (reservation price  $\text{RP}_i > 0$ );

$m_G$  = the slope of the generation ( $> 0$ ) (\$/MW<sup>2</sup>h);

$P_{G(i)}$  = supply (MW);

$N_g$  = number of generation buses.

At the operational point ( $P_i, G_i$ ), the apparent cost of production is expressed as:

$$C(i)_{P_{G(i)}} = \text{RP}_i \times P_{G(i)} + \frac{1}{2} m_G P_{G(i)}^2 \quad (13)$$

Likewise, the linear demand curve for the customer 'j' is expressed by:

$$P_j = \text{RP}_j + m_D P_{D(j)} \quad (14)$$

where  $P_j$  = the cost that 'j' is ready to pay (\$/MWh);

$\text{RP}_j$  = the intercept (reservation price  $\text{RP}_j > 0$ );

$m_D$  = the slope (\$/MW<sup>2</sup>h);

$P_{D(j)}$  = demand supply (MW);

$N_d$  = number of demand buses.

The consumer benefit can be presented as:

$$B(j)_{P_{D(j)}} = \text{RP}_j \times P_{D(j)} + \frac{1}{2} m_D P_{D(j)}^2 \quad (15)$$

Therefore, social welfare is interpreted as:

$$SW = \sum_{j=1}^{N_d} B(j)_{P_{D(j)}} - \sum_{i=1}^{N_g} C(i)_{P_{G(i)}} \quad (16)$$

It is revealed from Equation (16) that social welfare is the union of the generating cost of electricity and consumer benefits. Hence, to optimize social welfare, customer benefits must be maximized while minimizing power-generating costs. The maximizing of SW in this study is obtained by minimizing the objective function, as demonstrated in Equation (35) [38].

Locational marginal pricing is a very important part of mathematical modeling and is also termed nodal pricing (NP). This technique of setting pricing involves figuring out market-clearing prices at various transmission grid nodes or locations. It is constituted of the total of the marginal costs of transmission congestion, losses, and generation.

$$LMP = \text{Marginal cost of (congestion in transmission + losses + generation)} \quad (17)$$

### 2.7. Risk Assessment

In today's competitive environment, the necessity for risk assessment and management is becoming more and more crucial. In the realm of risk management, the approaches of value-at-risk (VaR) and conditional value-at-risk (CVaR) have grown in popularity. Based on probabilistic research and assurance confidence levels, both evaluation methods are built. VaR determines the maximum loss and level of confidence for a given period. CVaR is the most precise risk-measuring technique for calculating the potential loss in tail events since VaR does not reflect the amount of loss that may occur over the threshold. For instance, if VaR is estimated at a 95% confidence level, CVaR may be calculated considering the average of the 5% worst losses. The additional losses in the remaining 5% make up the CVaR. With a loss amount of  $(1 - \omega)$  percentile, VaR thus denotes the lowest loss, whereas CVaR gives the average loss components in the lower end of the loss distribution.

Here,  $g(x,y)$  is the loss related to the decision vector  $Q$ , which is to be chosen from a specific subset  $x$  of  $\dot{R}$  and the random vector  $y$  in  $\dot{R}$ . ' $\omega$ ' is the confidence level. The possibility that  $g(x,y)$  does not exceed a threshold  $\zeta$  is represented by  $p(y)$  and is thus expressed as [39]:

$$\psi(x, \zeta) = \int_{g(x,y) \leq \zeta} p(y) dy \quad (18)$$

Mathematically, the assurance level based on VaR and CVaR is represented by:

$$\zeta_{\omega}(x) = \min \{ \zeta \in \dot{R} : \psi(x, \zeta) \} \quad (19)$$

$$\varphi_{\omega}(x) = \frac{1}{1 - \omega} \left[ \left( \sum_{j=1}^{\omega} p_j - \omega \right) a_{j_{\omega}} + \sum_{j=j_{\omega}}^T p_j a_j \right] \quad (20)$$

where  $T$  = the quantity of attempts conducted under various circumstances, and loss points are arranged as:  $a_1 < a_2 < a_3 \dots \dots < a_T$ .

### 3. Objective Function

Let us consider an electricity network with ' $N_b$ ' buses, ' $N_g$ ' generators, and ' $N_l$ ' loads. Mathematically, the proposed approach's primary goals are to maximize societal welfare, reduce system generating costs, optimize investment costs for the UPFC, and limit investment costs for wind power generation. This research aims to increase social good and commercial gain while reducing generation costs and system risk in the case of cost imbalances. For the performance study of any renewable integrated power system, the imbalance cost concept must be taken. However, to the authors' knowledge, only a few researchers have taken this idea. The system operators use rewards and penalties to

create revenue; thus, the positive imbalance cost increases the system profit, while the negative imbalance cost decreases it. The maximization and minimization problems are the two objective functions in this study, respectively. The objective functions are modeled mathematically as:

### 3.1. The Objective Function (First Part)

$$P_{n(t)} = TR_{n(t)} + IMC_{n(t)} - TGC_{n(t)} \quad (21)$$

where  $P_{n(t)}$  = the n-th unit's total profit at a time 't',  $TR_{n(t)}$  = total revenue,  $IMC_{n(t)}$  = total imbalance cost, and  $TGC_{n(t)}$  = overall generation cost (containing the investment costs for wind power generation and thermal power generation).

The most crucial element in optimizing the profit of wind–thermal power plants under the newly deregulated electricity environment is the imbalance cost, which is the most significant consideration among the revenue, imbalance cost, and overall generating cost. The following is a description of the formulae for the total income, imbalance cost, and generation cost:

$$TR_{n(t)} = \sum_{i=1}^{N_g} P_{a,i(t)} \cdot LMP_{i(t)} \quad (22)$$

$$IMC_{m(t)} = \sum_{i=1}^{N_g} \left[ CR_{s(t)} + CR_{d(t)} \cdot \left( \frac{P_{f,i(t)}}{P_{a,i(t)}} \right)^2 \right] \cdot [P_{a,i(t)} - P_{f,i(t)}] \quad (23)$$

where  $P_{a,i(t)}$  = power generated with actual wind speed at a time 't' at the i-th generation bus,  $P_{f,i(t)}$  = power generated with the forecasted wind speed,  $CR_{s(t)}$  = charge rate (surplus), and  $CR_{d(t)}$  = charge rate (deficit).

$$TGC_{m(t)} = GC_{m(t)} + WGC_{m(t)} + Cost_{upfc} \quad (24)$$

where  $WGC$  = wind power investment cost. In a wind-incorporated deregulated setup, the wind-generated electricity is committed after being calculated based on the anticipated wind speed. If the actual wind speed data turns out to be different from the forecasted one, the fuel cell can aid to lessen the power required for operation to make up for the discrepancy. However, there may be expenditures associated with the imbalance caused by the discrepancy between the projected and actual wind speeds. Equation (23) shows the imbalance cost. The calculation methods for the charge rates (deficit and excess) are as follows:

$$CR_{d(t)} = (1 + \gamma) \cdot LMP_{i(t)}, \quad CR_{s(t)} = 0 \text{ when } P_{a,i(t)} < P_{f,i(t)} \quad (25)$$

$$CR_{s(t)} = (1 - \gamma) \cdot LMP_{i(t)}, \quad CR_{d(t)} = 0 \text{ when } P_{a,i(t)} > P_{f,i(t)} \quad (26)$$

$$CR_{s(t)} = CR_{d(t)} \text{ when } P_{a,i(t)} = P_{f,i(t)} \quad (27)$$

$$GC_{m(t)} = \sum_{i=1}^{N_g} x + y \cdot P_{a,i(t)} + z \cdot P_{a,i(t)}^2 \quad (28)$$

where  $LMP_{i(t)}$  = LMP at time 't' at the i-th bus,  $GC_{m(t)}$  = power generation cost of the thermal unit, and  $x$ ,  $y$ , and  $z$  are coefficients of the generation cost. The ICR, or imbalance charge rate (surplus or deficit), to MCP ratio is used to indicate the imbalance cost coefficient or ' $\gamma$ '. In the present work, the value of ' $\gamma$ ' is considered as 0.9.

### 3.2. The Objective Function (Second Part)

$$\text{Min. } \zeta_{\omega}(x) = \min \left\{ \zeta \in \dot{R} : \psi(x, \zeta) \right\} \quad (29)$$

$$\text{Min. } \varphi_{\omega}(x) = \frac{1}{1 - \omega} \left[ \left( \sum_{j=1}^{j(\omega)} P_j - \omega \right) a_{j(\omega)} + \sum_{j=j(\omega)}^T P_j a_j \right] \quad (30)$$

VaR and CvaR's functions are given in Equations (29) and (30), respectively. The evident reciprocal link between system risk and VaR and CvaR indicates that the degree of system risk will either be the highest or lowest Depending on whether VaR and CvaR have the smallest or largest negative values. As a result, extending from left to right of the curve (as illustrated in Figure 2), the system risk must be decreased or the VaR and CvaR values must be raised in a positive way. One of the main goals of this endeavor is to reduce system generating costs as much as possible. The rightmost tail of the curve, when the system profit is the maximum and the system generating cost is lowest, is where the VaR and CvaR are of most benefit. As a result, there is an inverse relationship between the VaR and CvaR and the system generation cost. Contrarily, system generating costs are negatively related to social welfare; thus, it rises when generation costs are reduced and falls when they are not. VaR and CVaR thus have a direct relationship with social well-being.

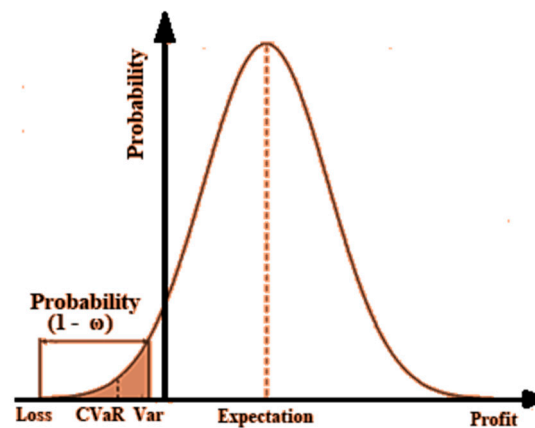


Figure 2. Illustration of VaR and CVaR.

The objective function has to be reduced suitably to satisfy all of the aforementioned requirements. The following is provided as the approach's objective function:

$$F = \sum_{i=1}^{N_g} C(i)_{P_{G(i)}} - \sum_{j=1}^{N_d} B(j)_{P_{D(j)}} + \sum_{m=1}^{N_{upfc}} C_m^{upfc} + \sum_{n=1}^{N_{wind}} C_n^{wind} \tag{31}$$

where  $N_{upfc}$  = the total number of UPFC devices, and  $N_{wind}$  = the total number of linked wind generators. It has been identified that the objective function is composed of societal welfare, UPFC investment costs, and WPG installation costs. The main purpose of the proposed strategy is to reduce the objective function (F), as shown in Equation (31). To meet this need, we have enhanced the consumer benefit curve, minimized the investment cost of the UPFC, and reduced the installation cost of the WPG. As a result, societal welfare improved significantly.

### 3.3. Constraints for OPF Solving

The optimum power flow (OPF) problem involves the constraints as mentioned below.

$$\sum_{i=1}^{N_g} P_{G,i} + P_w - P_L - P_D = 0 \tag{32}$$

$$P_L = \sum_{j=1}^{N_L} G_{i-j} \left[ |V_i|^2 + |V_j|^2 - 2|V_i||V_j| \cos(\delta_i - \delta_j) \right] \tag{33}$$

where  $P_{G,i}$  = generated power at the i-th generation unit,  $P_w$  = wind power,  $P_L$  = line loss,  $P_D$  = power demand,  $N_L$  = No. of transmission lines,  $G_{i-j}$  = line conductance of line between bus 'i' and 'j',  $\delta_i, |V_i|$  = phase angle and voltage magnitude of bus 'i', and  $\delta_j, |V_j|$  = phase angle and voltage magnitude of bus 'j'.

$$P_i - \sum_{k=1}^{N_b} |V_i V_k Y_{ik}| \cos(\theta_{ik} - \delta_i + \delta_k) = 0 \tag{34}$$

$$Q_i + \sum_{k=1}^{N_b} |V_i V_k Y_{ik}| \sin(\theta_{ik} - \delta_i + \delta_k) = 0 \quad (35)$$

where  $P_i$  = real power injected at the bus 'i',  $Q_i$  = reactive power injected at the bus 'i', and  $\theta_{ik}$ ,  $Y_{ik}$  = angle and magnitude of the element of the i-th row and the k-th column of the bus admittance matrix.

$$\text{Voltage : } V_{i(\min)} \leq V_i \leq V_{i(\max)} \text{ where } i = 1, 2, 3, 4, \dots N_b \quad (36)$$

$$\text{Angle : } \varphi_{i(\min)} \leq \varphi_i \leq \varphi_{i(\max)} \text{ where } i = 1, 2, 3, 4, \dots N_b \quad (37)$$

$$\text{Line flow (MVA) : } LF_l \leq LF_{l(\max)} \text{ where } l = 1, 2, 3, 4, \dots N_L \quad (38)$$

$$\text{Active power of bus : } PG_{i(\min)} \leq PG_i \leq PG_{i(\max)} \text{ where } i = 1, 2, 3, 4, \dots N_b \quad (39)$$

$$\text{Reactive power of bus : } QG_{i(\min)} \leq QG_i \leq QG_{i(\max)} \text{ where } i = 1, 2, 3, 4, \dots N_b \quad (40)$$

$$k_{\text{upfc}(\min)} \leq k_{\text{upfc}} \leq k_{\text{upfc}(\max)} \quad (41)$$

$$Q_{\text{upfc}(\min)} \leq Q_{\text{upfc}} \leq Q_{\text{upfc}(\max)} \quad (42)$$

where  $V_{i(\min)}$ ,  $V_{i(\max)}$  = lower and upper voltage limits of bus 'i',  $\varphi_{i(\min)}$ ,  $\varphi_{i(\max)}$  = lower and upper angle limits corresponding to the voltage of bus 'i',  $LF_l$ ,  $LF_{l(\max)}$  = actual and maximum line flow of line 'l',  $PG_{i(\min)}$ ,  $PG_{i(\max)}$  = lower and upper real power limits of bus 'i' and  $QG_{i(\min)}$ ,  $QG_{i(\max)}$  = lower and upper reactive power limits of bus 'i'.

This paper outlines a method to choose the best UPFC location and cost to accomplish the objective function's minimal value with all constraints (as mentioned in Equations (32)–(42)). In this method, optimization was carried out by positioning the UPFC, adjusting all control parameters within the predetermined bounds, and obtaining the best results. The UPFC will be placed at the optimal location where the objective function has the minimum value. For each prospective location of the UPFC, the optimum power flow has been repeatedly examined in this study.

### 3.4. Fuel Cell Constraints

Energy is stored using a hydrogen energy storage system made up of hydrogen tanks, an electrolyzer, and a fuel cell. Because electricity is less expensive during off-peak hours, energy is transformed into hydrogen by the electrolyzer and is preserved in hydrogen tanks. In the future, when energy prices are high during peak hours, a fuel cell can generate power using hydrogen that has accumulated. The following factors determine the electrolyzer's operation [40,41]:

$$E_{\text{elz}(\min)} \leq E_{\text{elz}} \leq E_{\text{elz}(\max)} \quad (43)$$

$$E_{\text{H}_2(\min)}^P \leq E_{\text{H}_2}^P \leq E_{\text{H}_2(\max)}^P \quad (44)$$

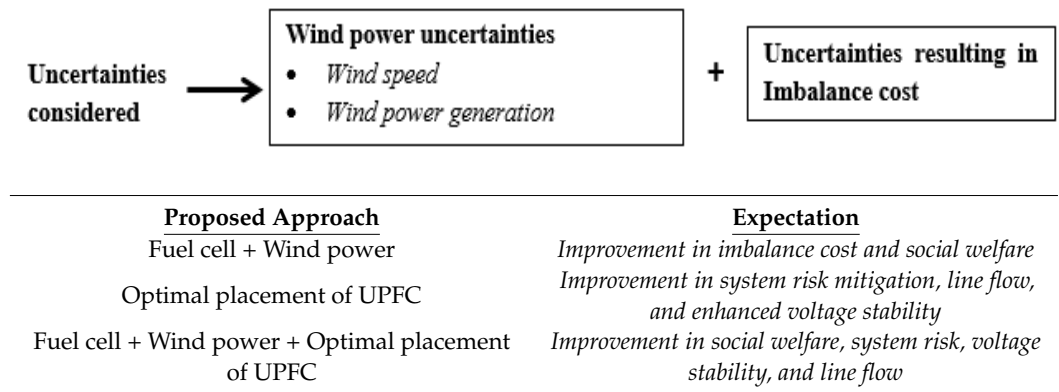
The following factors determine the fuel cell's operation:

$$E_{\text{fc}(\min)} \leq E_{\text{fc}} \leq E_{\text{fc}(\max)} \quad (45)$$

$$f_{\text{H}_2(\min)}^{\text{con}} \leq f_{\text{H}_2}^{\text{con}} \leq f_{\text{H}_2(\max)}^{\text{con}} \quad (46)$$

## 4. Proposed Approach

This research illustrates an optimization strategy for allocating UPFC devices in the wind power-integrated deregulated electricity system. This paper suggests a way for assessing system risk and social benefit in a wind–fuel cell-incorporated deregulated power system. For 24 h situations, the technique takes into account the implications of a disagreement between the anticipated and actual wind speeds.



#### 4.1. Algorithm for Placing UPFC

This approach finds the objective function for each situation by placing a UPFC in each line of the system, separately. In the end, UPFCs are placed along the lines with the least objective function values. A flowchart showing the said approach is shown in Figure 3, where ‘ $N_{upfc}$ ’ indicates the number of UPFCs, ‘ $WG_{cost}$ ’ indicates the cost of wind generation, and ‘ $\Delta k_{upfc}$ ’ indicates the increment in ‘ $k_{upfc}$ ’.

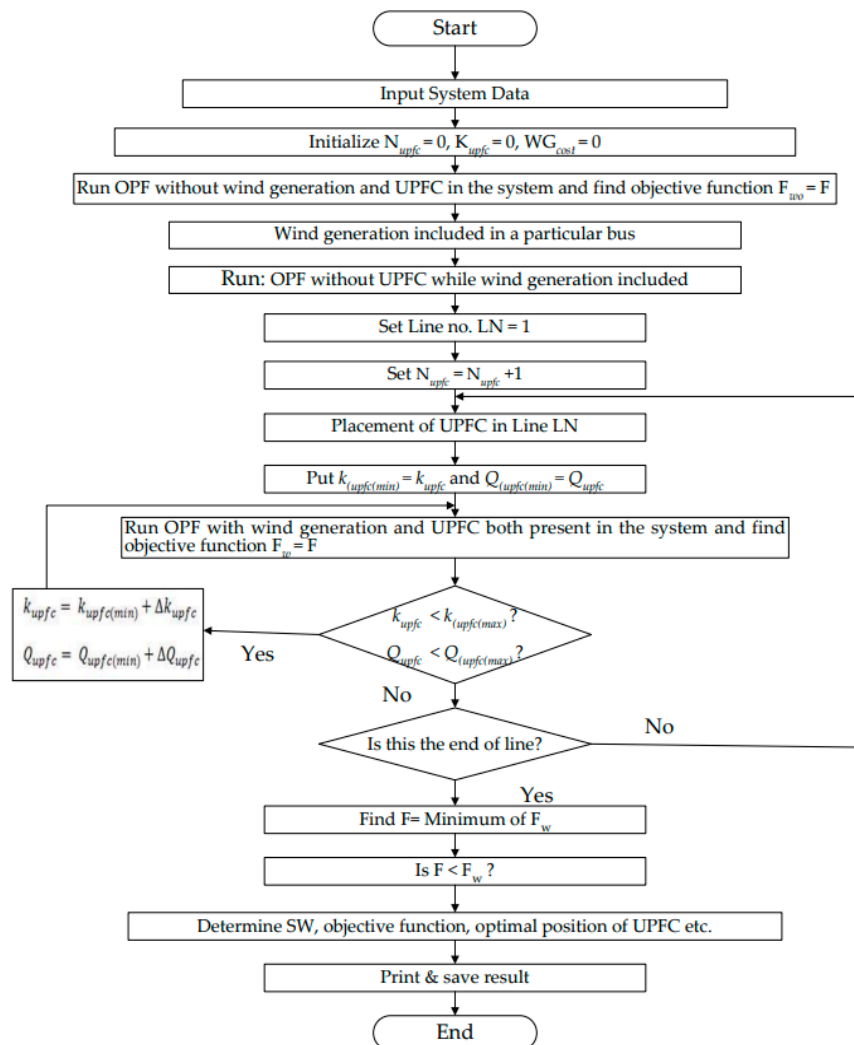


Figure 3. Flowchart for positioning UPFCs most effectively.

4.2. Application of the Proposed Approach

This work has been conducted using a modified IEEE 30-bus system to evaluate the efficacy of the suggested technique. MATPOWER was used in this study to find the solution to the optimal power flow problem. Flowcharts of profit calculation and risk assessment are shown in Figures 4 and 5.

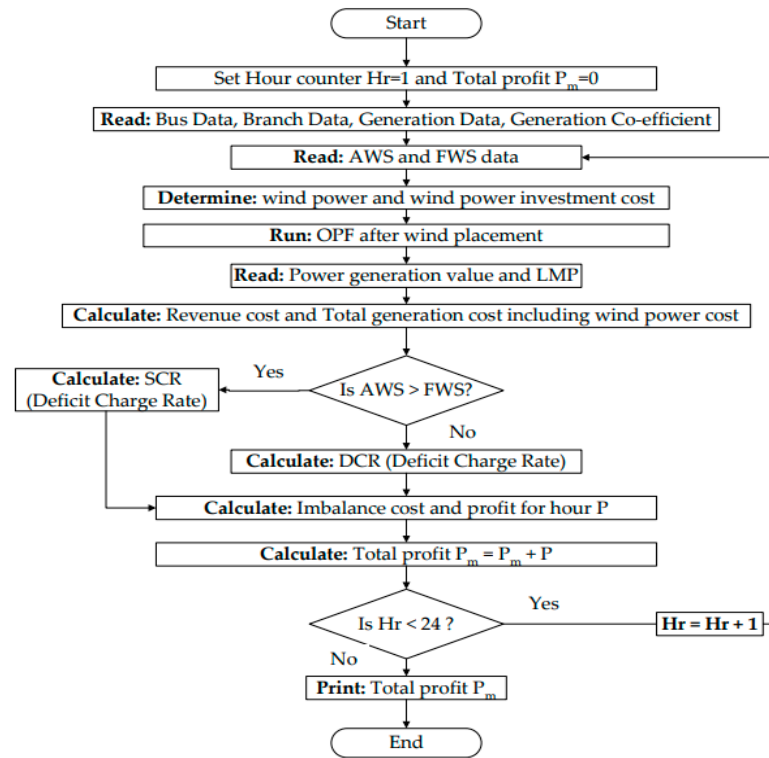


Figure 4. Profit-calculating flowchart.

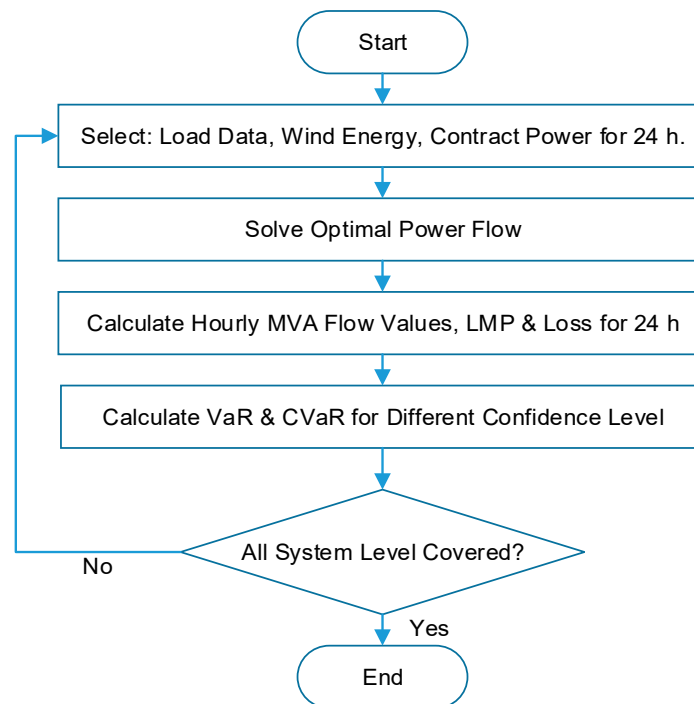


Figure 5. Flowchart for risk assessment.

#### 4.3. Integration of a UPFC and a WPG on a Modified IEEE 30-Bus System

In this research, a modified IEEE 30-bus system is utilized to examine how the recommended approach works. The test system's information is gathered from [42,43]. The OPF problem was initially solved using SQP, and several meta-heuristic optimization techniques were subsequently applied for comparison studies.

### 5. Results and Analysis

Three system scenarios were evaluated to substantiate the suggested technique and demonstrate the effects of a WPG and a UPFC in the system:

- Regulated system;
- Deregulated system with single-demand bus auction bidding;
- Deregulated system with double-demand bus auction bidding.

In addition, the system was analyzed considering the following cases:

- System performance in the absence of a WPG and a UPFC;
- System performance when only a WPG is present;
- System performance when a WPG is present and the UPFC is optimally located.

#### 5.1. Case 1: Performance of the System in the Absence of a WPG

The OPF in a modified IEEE 30-bus system in the absence of a wind generator has been performed. The generating cost, system revenue, and profit for various systems are displayed in Figure 6. The data for all generators for the various cases under consideration are provided in Table 3. It has been observed that demand-side bidding reduces system generating costs, directly benefiting power consumers. Demand-side bidding suggests that the present electricity system may go ahead with more deregulation. As additional buses are added to the demand-side bidding (DSB), the generating costs decrease and LMP increases, as can be seen from the results displayed in Figure 7. Various scenarios' voltage and transmission line losses are shown in Figures 8 and 9. Both tables exhibit higher improvements after the double-demand-side bidding.

Demand-side bidding (DSB) is used for the modified IEEE 30-bus system at bus number 4 for a single-bus bidding and at bus numbers 4 and 21 for a double-bus bidding. To allow the load and generation sides some flexibility, this analysis has taken into account both generation- and demand-side biddings. Figure 10 depicts the single-line diagram for a modified IEEE 30-bus system with the bidding structure.

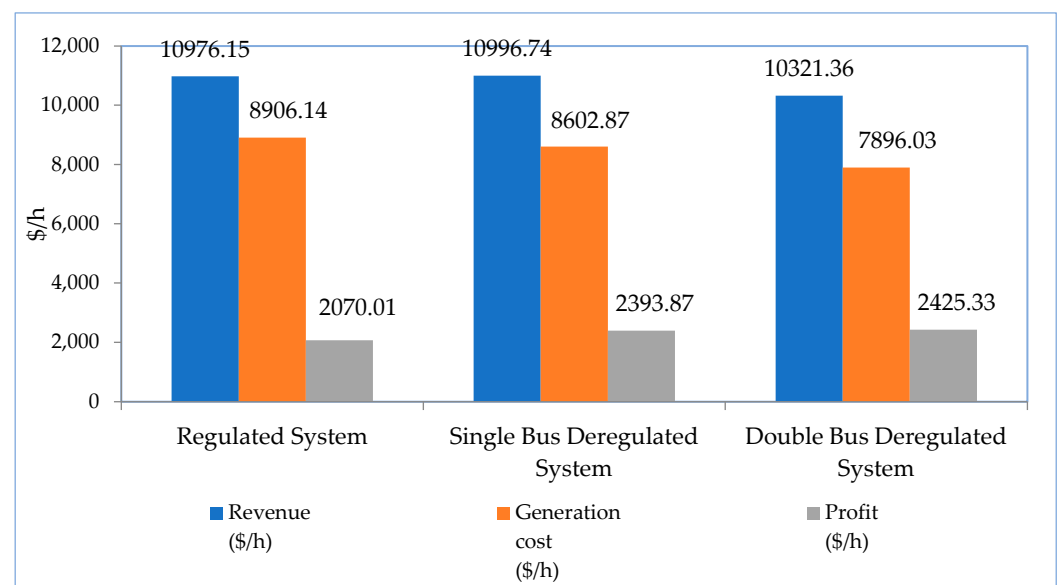


Figure 6. Generation cost, revenue, and profit of various systems.

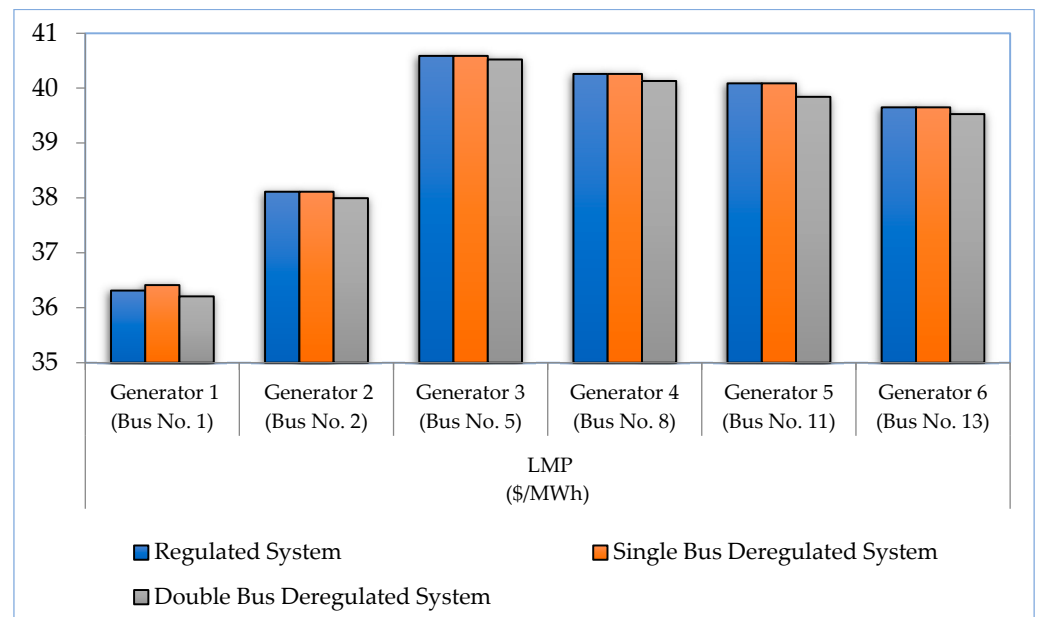


Figure 7. Comparison of the LMP of various systems.

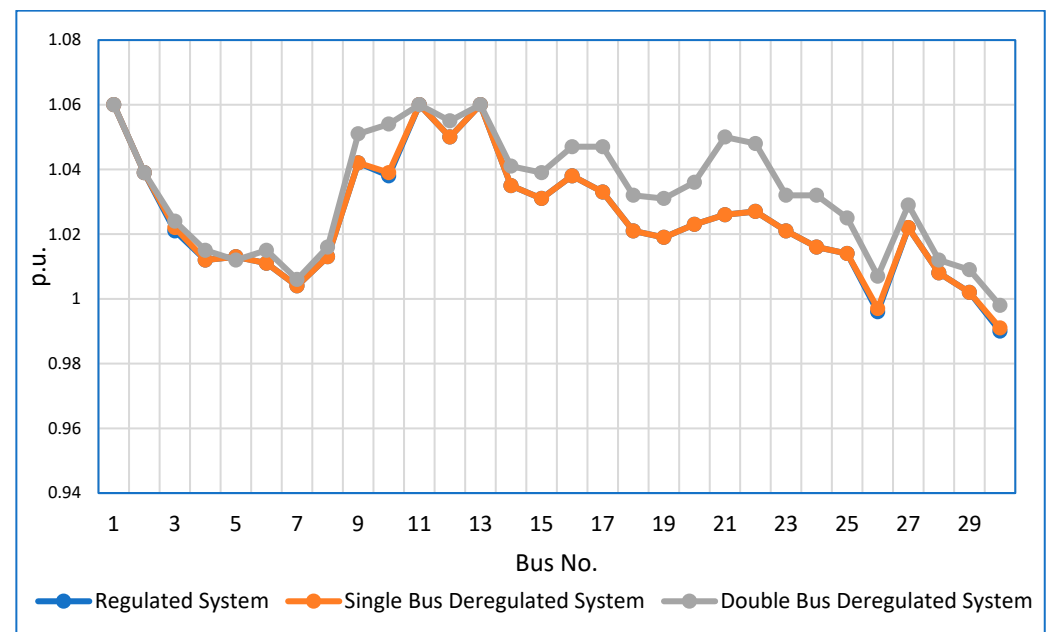


Figure 8. Bus voltage (in p.u.) comparison.

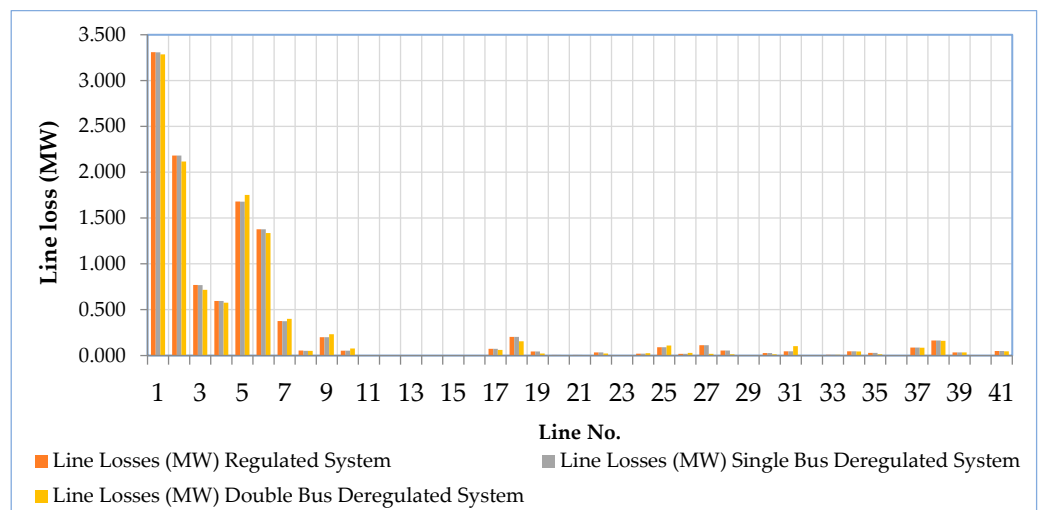


Figure 9. Comparison of line losses.

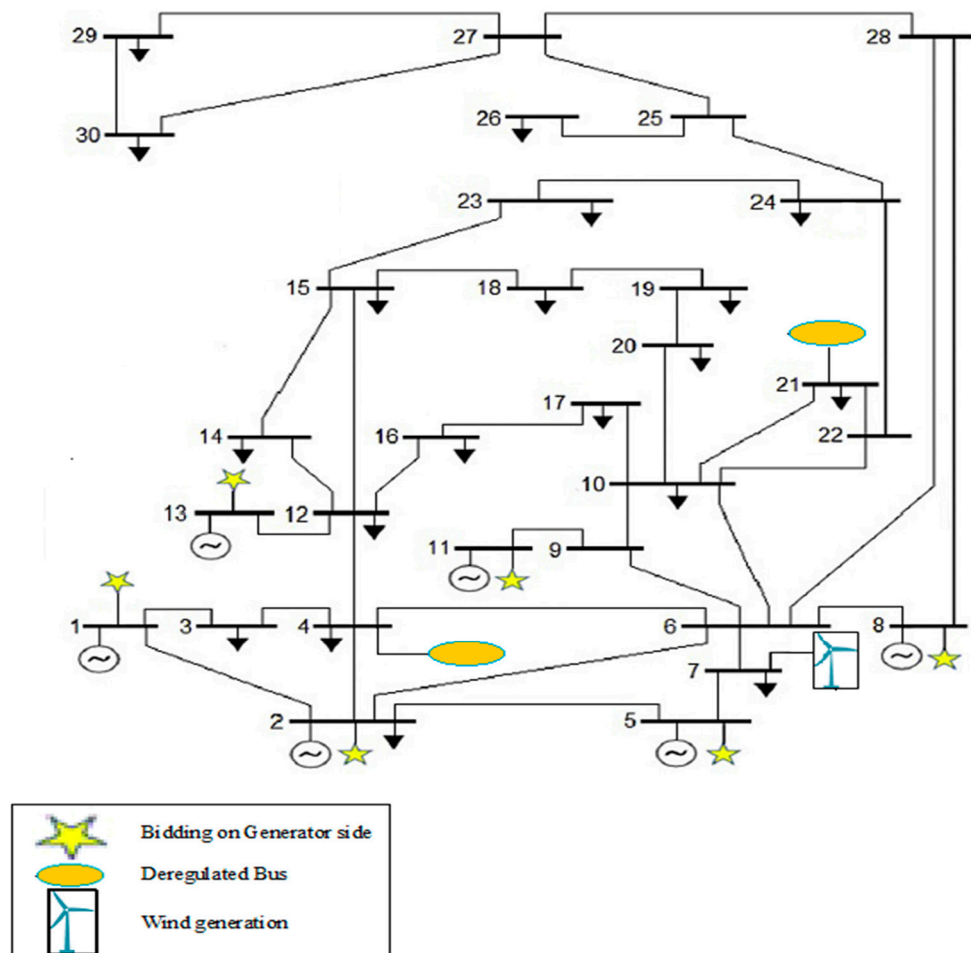


Figure 10. A single-line schematic of the modified IEEE 30-bus system.

Demand-side and generator-side bidding have both proven effective in the deregulated power scenario. As a result, compared to the regulated system, the power scheduling procedure is altered. Customers usually become financial gainers because the electrical sector is hugely competitive. The system currently includes many generation companies, which has increased the competition and quality of the power. For these reasons, after

the system is changed to a deregulated system, significant positive changes in the system voltage profile as well as in transmission line losses are observed.

From Figure 8, it is seen that the system voltage profile reaches very near to the desired 1 p.u. after the implementation of the deregulated environment compared to the regulated one. The graph indicates a more stable system condition with the deregulated environment. Table 3 shows the optimal generation capacity of each generator considering all three chosen cases. It can be seen that the generation from Generator 6 is zero for all conditions. So, it has not been included in Table 3.

Table 3. Comparison of generation data of various systems.

| Wind Speed (m/s) | Generator 1      |                               | Generator 2                   |                  | Generator 3                   |                               | Generator 4      |                               | Generator 5                   |                  |                               |                               |      |      |   |
|------------------|------------------|-------------------------------|-------------------------------|------------------|-------------------------------|-------------------------------|------------------|-------------------------------|-------------------------------|------------------|-------------------------------|-------------------------------|------|------|---|
|                  | Regulated System | Single-Bus Deregulated System | Double-Bus Deregulated System | Regulated System | Single-Bus Deregulated System | Double-Bus Deregulated System | Regulated System | Single-bus Deregulated System | Double-Bus Deregulated System | Regulated System | Single-Bus Deregulated System | Double-Bus Deregulated System |      |      |   |
| 1.67             | 212.16           | 212.18                        | 210.78                        | 36.22            | 36.22                         | 35.98                         | 28.99            | 29                            | 25.65                         | 12.67            | 12.66                         | 6.24                          | 4.09 | 4.05 | 0 |
| 1.94             | 212.12           | 212.14                        | 210.73                        | 36.21            | 36.21                         | 35.97                         | 28.74            | 28.78                         | 25.41                         | 12.48            | 12.5                          | 6.04                          | 3.88 | 3.87 | 0 |
| 2.22             | 212.07           | 212.08                        | 210.66                        | 36.2             | 36.2                          | 35.96                         | 28.49            | 28.5                          | 25.11                         | 12.29            | 12.29                         | 5.78                          | 3.66 | 3.63 | 0 |
| 2.50             | 212              | 212.01                        | 210.58                        | 36.19            | 36.19                         | 35.95                         | 28.12            | 28.14                         | 24.71                         | 12.02            | 12.02                         | 5.45                          | 3.35 | 3.31 | 0 |
| 2.78             | 211.91           | 211.93                        | 210.48                        | 36.17            | 36.17                         | 35.93                         | 27.67            | 27.68                         | 24.22                         | 11.68            | 11.68                         | 5.04                          | 2.96 | 2.93 | 0 |
| 3.06             | 211.81           | 211.82                        | 210.36                        | 36.15            | 36.15                         | 35.91                         | 27.11            | 27.13                         | 23.62                         | 11.26            | 11.26                         | 4.53                          | 2.49 | 2.45 | 0 |
| 3.33             | 211.68           | 211.7                         | 210.21                        | 36.13            | 36.13                         | 35.88                         | 26.44            | 26.46                         | 22.9                          | 10.76            | 10.76                         | 3.93                          | 1.93 | 1.88 | 0 |
| 3.61             | 211.53           | 211.55                        | 210.03                        | 36.1             | 36.1                          | 35.85                         | 25.64            | 25.67                         | 22.05                         | 10.15            | 10.17                         | 3.21                          | 1.3  | 1.22 | 0 |
| 3.89             | 211.33           | 211.36                        | 209.82                        | 36.07            | 36.07                         | 35.81                         | 24.68            | 24.72                         | 21.06                         | 9.38             | 9.43                          | 2.38                          | 0.67 | 0.54 | 0 |
| 4.17             | 211.07           | 211.1                         | 209.58                        | 36.02            | 36.02                         | 35.77                         | 23.49            | 23.53                         | 19.91                         | 8.35             | 8.38                          | 1.43                          | 0.21 | 0.11 | 0 |
| 4.44             | 210.74           | 210.75                        | 209.28                        | 35.96            | 35.96                         | 35.72                         | 22.05            | 22.05                         | 18.55                         | 6.98             | 6.95                          | 0.5                           | 0    | 0.01 | 0 |
| 4.72             | 210.33           | 210.34                        | 208.85                        | 35.89            | 35.89                         | 35.64                         | 20.34            | 20.34                         | 16.78                         | 5.31             | 5.29                          | 0.05                          | 0    | 0    | 0 |

5.2. Case 2: System Performance with a WPG but without Considering the Imbalance Cost

SQP has been employed to estimate the optimum power flow, and bus number 4 has been chosen at random as the location for the wind generator. When computing the entire generating cost, which also includes the cost of generation of the thermal system, the wind investment cost is taken into account. For numerous systems with varied specified wind speeds, Figure 11 displays the revenue costs and overall generating costs. The system may experience a drop in the overall generation cost and a rise in profit as deregulation approaches.

Figure 12 displays a comparison of system profits at various wind speeds. Adding more wind power into the system results in a better profit. Social welfare and system generation costs are inversely related. It is evident in this instance that adding wind farms to the system reduces generation costs, maximizing societal benefits.

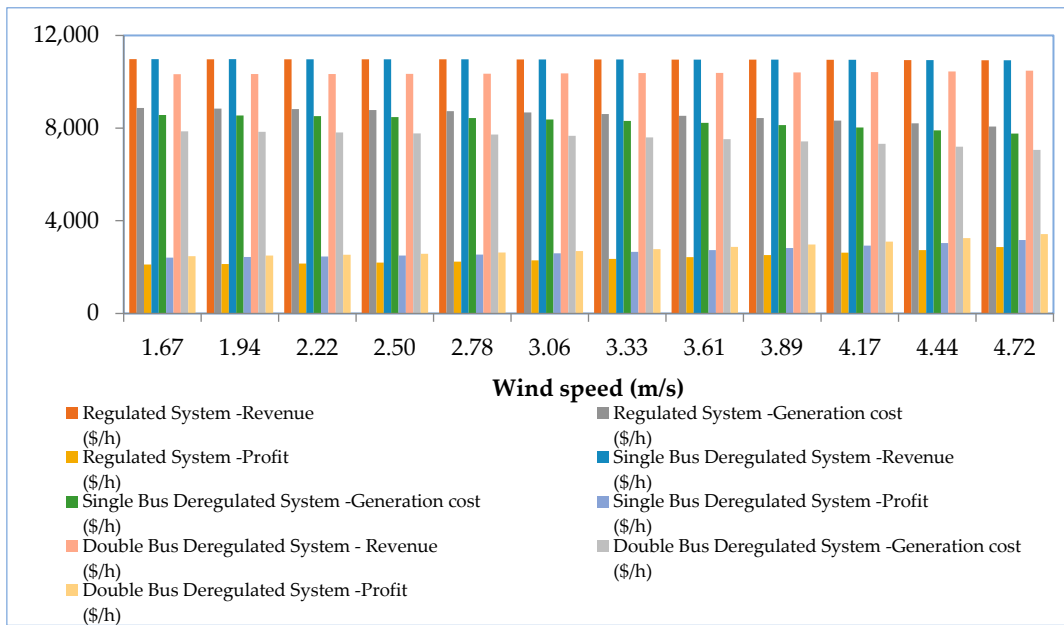


Figure 11. Generation cost, revenue, and profit for various systems at different wind speeds.

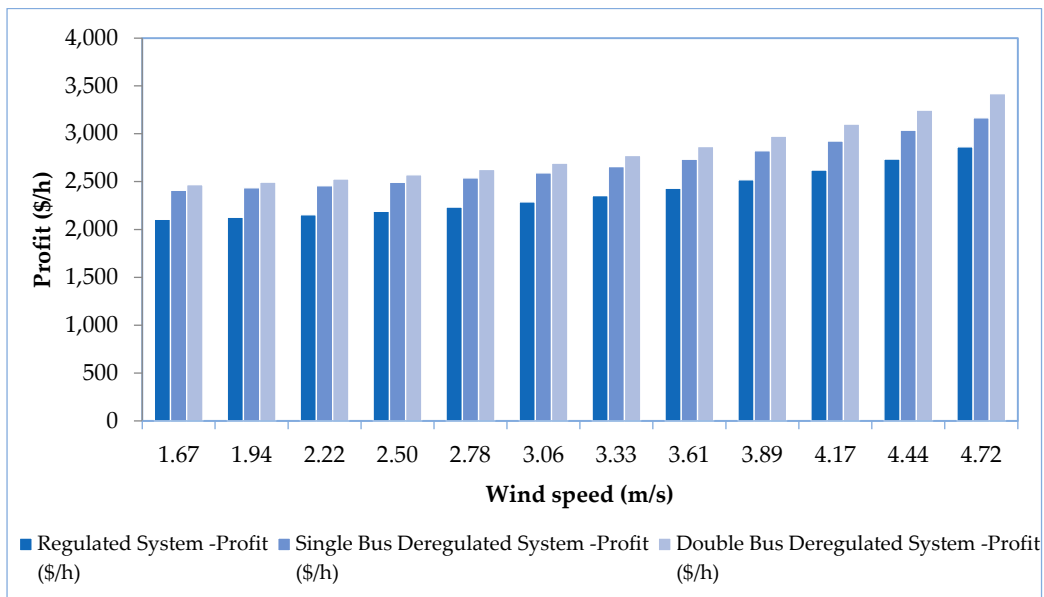


Figure 12. Comparison of profit for different wind speeds in various cases.

5.3. Case 3: System Performance with a WPG and Considering the Imbalance Cost

With a wind-integrated electrical system, the idea of the imbalance cost accounts for the implications of variable wind speeds on profit. The location of the wind generator inside the system was arbitrary. The wind generator in this instance was located on bus number 7, and OPF was performed for each wind datapoint while taking into consideration all of the limitations specified in Equations (32)–(40). The cost of thermal generation is estimated along with the overall cost of generating electricity after the wind generator is placed, taking the cost of the wind power investment into account. The generation cost of the thermal system fluctuates according to the circumstance due to producing rescheduling.

Figure 13 shows that the generation cost of the thermal units decreases as wind speed/wind power rises. Table 4 indicates that LMP improves with the increase in wind speed. In all circumstances, this lowers the thermal power generation cost while enhancing wind power.

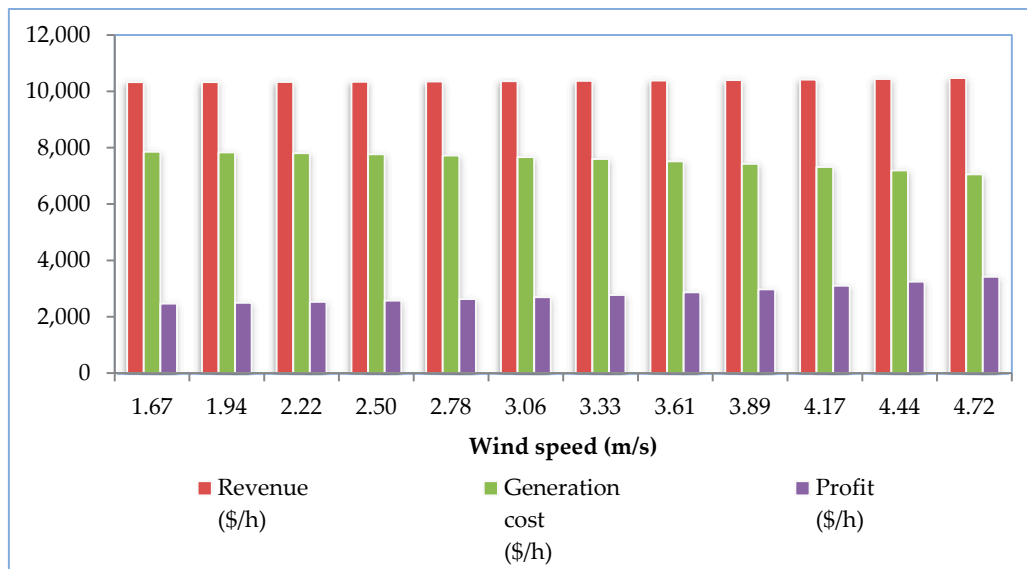


Figure 13. Comparison of revenue, generation cost, and profit at different wind speeds.

Table 4. Generation and LMP calculations for the modified IEEE 30-bus system after wind placement.

| Wind Speed (m/s) | Gen 1           |              | Gen 2           |              | Gen 3           |              | Gen 4           |              | Gen 5           |              | Gen 6           |              |
|------------------|-----------------|--------------|-----------------|--------------|-----------------|--------------|-----------------|--------------|-----------------|--------------|-----------------|--------------|
|                  | Generation (\$) | LMP (\$/MWh) |
| 1.67             | 210.78          | 36.20        | 35.98           | 37.99        | 25.65           | 40.51        | 6.24            | 40.13        | 0.00            | 39.88        | 0.00            | 39.52        |
| 1.94             | 210.73          | 36.20        | 35.97           | 37.99        | 25.41           | 40.51        | 6.04            | 40.12        | 0.00            | 39.83        | 0.00            | 39.51        |
| 2.22             | 210.66          | 36.19        | 35.96           | 37.98        | 25.11           | 40.50        | 5.78            | 40.12        | 0.00            | 39.82        | 0.00            | 39.51        |
| 2.50             | 210.58          | 36.19        | 35.95           | 37.97        | 24.71           | 40.49        | 5.45            | 40.11        | 0.00            | 39.81        | 0.00            | 39.50        |
| 2.78             | 210.48          | 36.18        | 35.93           | 37.97        | 24.22           | 40.48        | 5.04            | 40.10        | 0.00            | 39.80        | 0.00            | 39.48        |
| 3.06             | 210.36          | 36.17        | 35.91           | 37.95        | 23.62           | 40.47        | 4.53            | 40.09        | 0.00            | 39.79        | 0.00            | 39.47        |
| 3.33             | 210.21          | 36.16        | 35.88           | 37.94        | 22.90           | 40.46        | 3.93            | 40.08        | 0.00            | 39.78        | 0.00            | 39.45        |
| 3.61             | 210.03          | 36.14        | 35.85           | 37.92        | 22.05           | 40.44        | 3.21            | 40.06        | 0.00            | 39.76        | 0.00            | 39.43        |
| 3.89             | 209.82          | 36.13        | 35.81           | 37.91        | 21.06           | 40.42        | 2.38            | 40.05        | 0.00            | 39.74        | 0.00            | 39.41        |
| 4.17             | 209.58          | 36.11        | 35.77           | 37.88        | 19.91           | 40.40        | 1.43            | 40.03        | 0.00            | 39.72        | 0.00            | 39.38        |
| 4.44             | 209.28          | 36.09        | 35.72           | 37.86        | 18.55           | 40.37        | 0.50            | 40.00        | 0.00            | 39.69        | 0.00            | 39.34        |
| 4.72             | 208.85          | 36.05        | 35.64           | 37.82        | 16.78           | 40.34        | 0.05            | 39.95        | 0.00            | 39.64        | 0.00            | 39.29        |

The mismatch between real wind speed data and predictions is represented by the system’s imbalance cost. The imbalance cost (negative) is largest when the disagreement between the predicted and actual wind speeds is greatest. A deficit charge rate is attained when the actual wind speed exceeds the anticipated wind speed, while a surplus charge rate is attained when the actual wind speed is lower than the anticipated wind speed. By taking the deficit and excess charge rates into consideration, we can determine the total imbalance cost of the electrical system. If the projected and actual wind speeds match, there is no cost associated with the imbalance. There is a certain number of hours in city situations where the cost of the imbalance is zero, as shown in Table 5. It is the outcome of the precise wind speed forecasts. The 24 h interval system’s imbalance cost is also

shown in Table 5 for each selected location in India. The “positive” imbalance cost means that GENCOs are rewarded by the ISO for supplying more power as opposed to being penalized by the ISO for providing inadequate power, which contrasts with the “negative” imbalance cost.

**Table 5.** Imbalance cost (in \$/h) calculations for 24 h.

| Hour | Delhi  | Mumbai    | Hour | Delhi    | Mumbai    |
|------|--------|-----------|------|----------|-----------|
| 1    | 0      | 0         | 13   | 3.0727   | 6.3861    |
| 2    | 4.189  | 3.0727    | 14   | 0        | 6.5408    |
| 3    | 4.189  | −48.4454  | 15   | 0        | 6.4891    |
| 4    | 4.189  | 0         | 16   | 0        | 0         |
| 5    | 2.4329 | 0         | 17   | 0        | −404.6408 |
| 6    | 2.4329 | −48.4454  | 18   | 0        | −671.0034 |
| 7    | 4.189  | −48.4454  | 19   | 0        | −499.7596 |
| 8    | 2.4329 | −62.157   | 20   | 0        | −285.583  |
| 9    | 5.2252 | −77.2631  | 21   | 0        | −77.2631  |
| 10   | 6.7857 | −171.9853 | 22   | −48.4454 | −62.157   |
| 11   | 4.189  | 0         | 23   | −48.4454 | −48.4454  |
| 12   | 4.189  | 9.6045    | 24   | 0        | 0         |

#### 5.4. Estimated Profit throughout the Day

An electrical system’s profit at any moment is primarily determined by its revenue cost and production cost. A comparison between projected and actual wind speeds has been conducted in this study to include the imbalance cost factors in the system’s profit calculation. Table 6 displays the profit values for 24 h for each site when the system is operating in a deregulated electricity environment. By lessening the negative effects of imbalance costs, the profit is raised. After the WF was installed in the system and the predicted and actual wind speed data were analyzed, Mumbai was found to have the highest profit due to more accurate forecasts of wind speed, whereas Delhi recorded the lowest profit since forecasting was less accurate.

**Table 6.** Profit (in \$/h) estimation of the system for 24 h.

| Hour | Delhi    | Mumbai   | Hour | Delhi    | Mumbai   |
|------|----------|----------|------|----------|----------|
| 1    | 2527.760 | 2527.760 | 13   | 2574.730 | 2981.502 |
| 2    | 2531.949 | 2574.730 | 14   | 2571.657 | 3107.078 |
| 3    | 2531.949 | 2445.352 | 15   | 2571.657 | 3252.557 |
| 4    | 2531.949 | 2527.760 | 16   | 2571.657 | 3246.068 |
| 5    | 2530.192 | 2527.760 | 17   | 2527.760 | 2695.897 |
| 6    | 2530.192 | 2445.352 | 18   | 2493.797 | 2101.325 |
| 7    | 2531.949 | 2445.352 | 19   | 2493.797 | 2126.559 |
| 8    | 2530.192 | 2465.603 | 20   | 2493.797 | 2286.074 |
| 9    | 2576.883 | 2494.394 | 21   | 2493.797 | 2494.394 |
| 10   | 2578.443 | 2399.672 | 22   | 2445.352 | 2465.603 |
| 11   | 2531.949 | 2692.884 | 23   | 2445.352 | 2445.352 |
| 12   | 2531.949 | 2875.584 | 24   | 2527.760 | 2493.797 |

5.5. Profit Comparison following WF Installation, Taking AWS and FWS into Account

This case provides an overview of the general conclusions and findings drawn as an outcome of the deliberate work. Figure 14 shows a profit comparison while accounting for numerous scenarios for all the selected sites. It is clear that, following wind placement, profit is enhanced (Figure 15) for every site, but due to the presence of imbalance costs, profit is lowered for every location. Since wind flow is unpredictable, contracts between market participants in a deregulated power market must take this into account. When employing wind power, the system is more secure and adaptable thanks to wind speed predictions. In the event of AWS and FWS mismatch, profit can be reduced. This is supported by the data in Tables 7 and 8. A summary of the variations in the imbalance costs for the various instances taken into consideration for 24 h is shown in Figure 16.

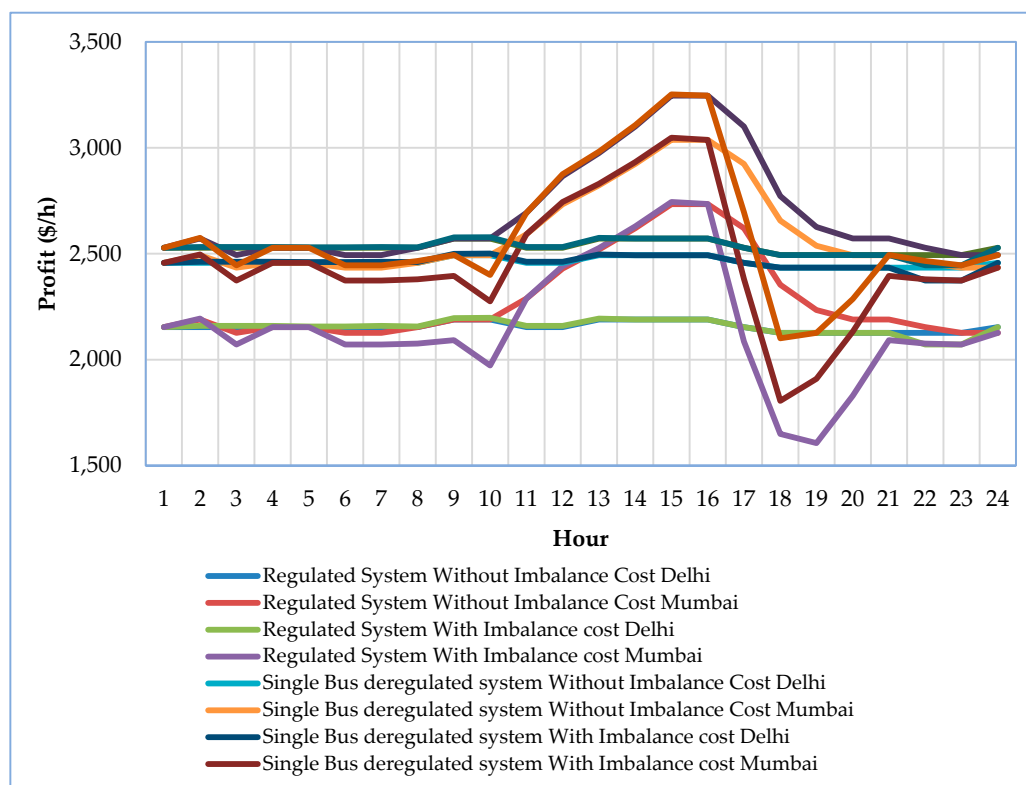


Figure 14. Profit comparison of the two cities for 24 h.

Table 7. Comparison of hourly profit (\$/h) of Mumbai considering imbalance costs.

| Hour | Regulated System | Single Bus Deregulated System | Double Bus Deregulated System | Hour | Regulated System | Single Bus Deregulated System | Double Bus Deregulated System |
|------|------------------|-------------------------------|-------------------------------|------|------------------|-------------------------------|-------------------------------|
| 1    | 2153.898         | 2457.195                      | 2527.760                      | 13   | 2526.688         | 2829.709                      | 2981.502                      |
| 2    | 2193.581         | 2496.683                      | 2574.730                      | 14   | 2629.028         | 2932.696                      | 3107.078                      |
| 3    | 2071.723         | 2373.628                      | 2445.352                      | 15   | 2744.802         | 3048.138                      | 3252.557                      |
| 4    | 2153.898         | 2457.195                      | 2527.760                      | 16   | 2734.410         | 3037.441                      | 3246.068                      |
| 5    | 2153.898         | 2457.195                      | 2527.760                      | 17   | 2085.540         | 2380.981                      | 2695.897                      |
| 6    | 2071.723         | 2373.628                      | 2445.352                      | 18   | 1649.467         | 1805.740                      | 2101.325                      |
| 7    | 2071.723         | 2373.628                      | 2445.352                      | 19   | 1606.301         | 1909.194                      | 2126.559                      |
| 8    | 2075.577         | 2378.883                      | 2465.603                      | 20   | 1829.428         | 2132.467                      | 2286.074                      |
| 9    | 2091.728         | 2395.522                      | 2494.394                      | 21   | 2091.728         | 2395.522                      | 2494.394                      |

Table 7. Cont.

| Hour | Regulated System | Single Bus Deregulated System | Double Bus Deregulated System | Hour | Regulated System | Single Bus Deregulated System | Double Bus Deregulated System |
|------|------------------|-------------------------------|-------------------------------|------|------------------|-------------------------------|-------------------------------|
| 10   | 1972.335         | 2275.447                      | 2399.672                      | 22   | 2075.577         | 2378.883                      | 2465.603                      |
| 11   | 2288.263         | 2591.590                      | 2692.884                      | 23   | 2071.723         | 2373.628                      | 2445.352                      |
| 12   | 2441.456         | 2744.366                      | 2875.584                      | 24   | 2126.452         | 2434.508                      | 2493.797                      |

Table 8. Comparison of hourly profit (\$/h) of Delhi considering imbalance costs.

| Hour | Regulated System | Single Bus Deregulated System | Double Bus Deregulated System | Hour | Regulated System | Single Bus Deregulated System | Double Bus Deregulated System |
|------|------------------|-------------------------------|-------------------------------|------|------------------|-------------------------------|-------------------------------|
| 1    | 2153.898         | 2457.195                      | 2527.760                      | 13   | 2193.581         | 2496.683                      | 2574.730                      |
| 2    | 2159.079         | 2462.349                      | 2531.949                      | 14   | 2189.747         | 2492.862                      | 2571.657                      |
| 3    | 2159.079         | 2462.349                      | 2531.949                      | 15   | 2189.747         | 2492.862                      | 2571.657                      |
| 4    | 2159.079         | 2462.349                      | 2531.949                      | 16   | 2189.747         | 2492.862                      | 2571.657                      |
| 5    | 2156.641         | 2460.228                      | 2530.192                      | 17   | 2153.898         | 2457.195                      | 2527.760                      |
| 6    | 2156.641         | 2460.228                      | 2530.192                      | 18   | 2126.452         | 2434.508                      | 2493.797                      |
| 7    | 2159.079         | 2462.349                      | 2531.949                      | 19   | 2126.452         | 2434.508                      | 2493.797                      |
| 8    | 2156.641         | 2460.228                      | 2530.192                      | 20   | 2126.452         | 2434.508                      | 2493.797                      |
| 9    | 2195.966         | 2499.319                      | 2576.883                      | 21   | 2126.452         | 2434.508                      | 2493.797                      |
| 10   | 2198.105         | 2501.179                      | 2578.443                      | 22   | 2071.723         | 2373.628                      | 2445.352                      |
| 11   | 2159.079         | 2462.349                      | 2531.949                      | 23   | 2071.723         | 2373.628                      | 2445.352                      |
| 12   | 2159.079         | 2462.349                      | 2531.949                      | 24   | 2153.898         | 2457.195                      | 2527.760                      |

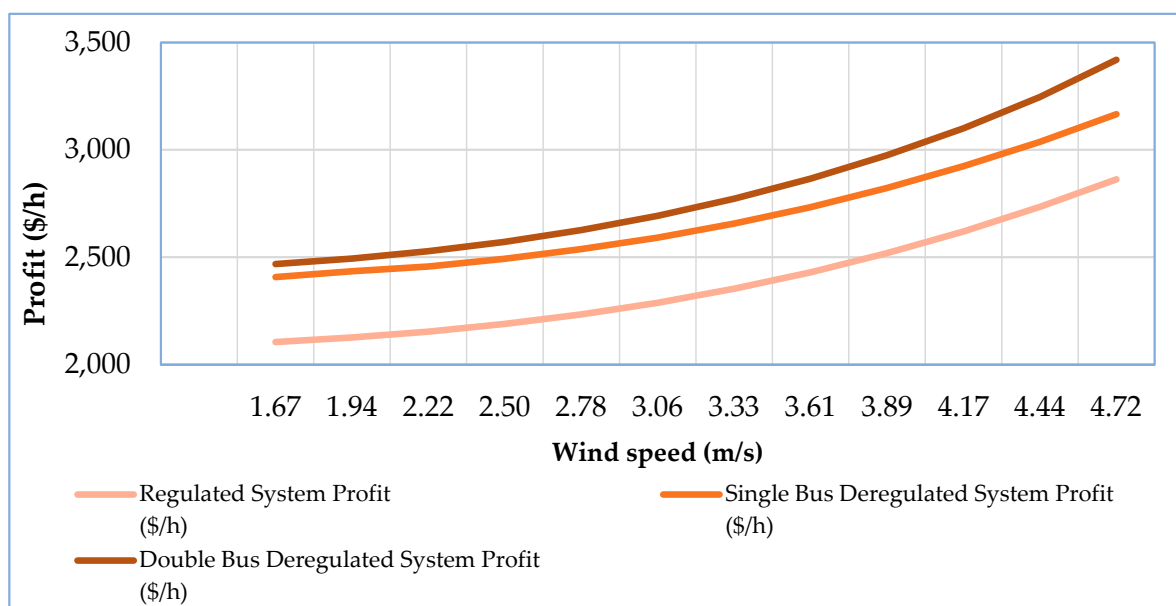
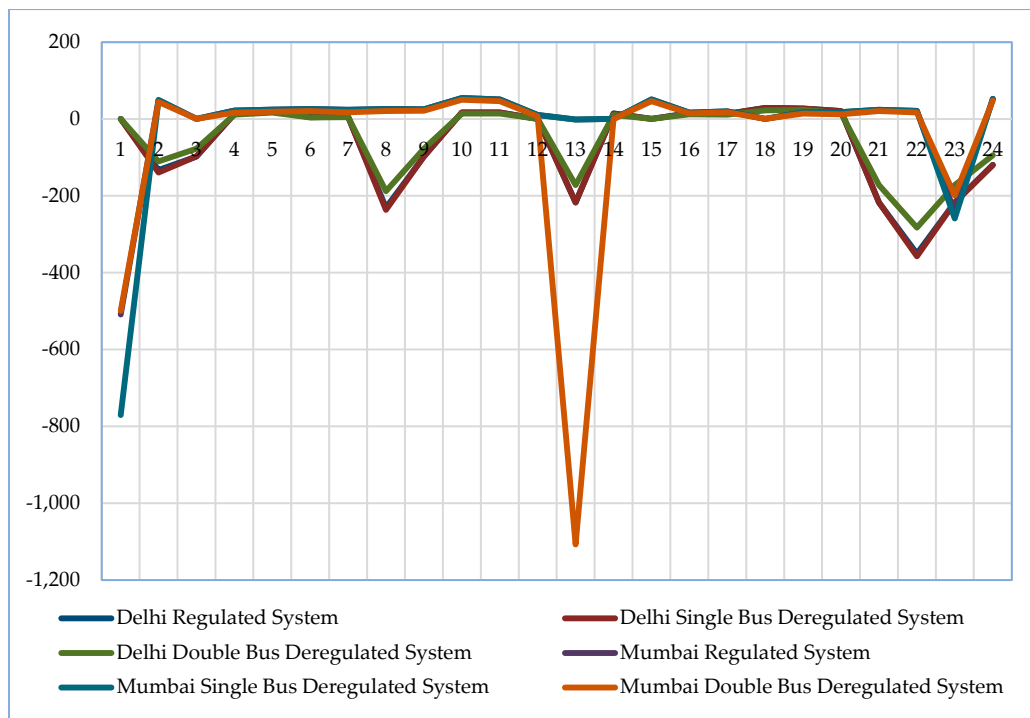


Figure 15. Variation in profit after wind placement in different systems.



**Figure 16.** Imbalance cost (\$/h) analysis of Delhi and Mumbai for 24 h.

#### 5.6. Case 4: Performance of System with a UPFC and Wind Farm Installation

Using this test system, six generators, thirty buses, forty-one transmission lines, and nineteen loads were employed to assess the efficacy of the suggested strategy. The system information is available in [43]. Here, three test system situations were looked at to validate the methodology that was described and to demonstrate the effects of WPGs and UPFCs:

- (1) Performance of the system in the absence of a WPG and a UPFC.
- (2) Performance of a WPG-based system without a UPFC.
- (3) Performance of a WPG-based system with optimal UPFC placement.

First, OPF was performed without a WPG or a UPFC, and the total generating cost was calculated to be 550.067 \$/h. The 23.04 MW wind generator is connected to bus number 7 in the system being illustrated. The hourly investment cost of a 1 MW wind power generator is \$3.75 (approx.) according to [25].

In this instance, the modified IEEE 30-bus system's OPF was obtained without WPG and UPFC placement, and the resulting total generation cost was determined to be \$550.0674 per hour. Then, the 23.04 MW wind power generator was coupled to bus number 7 in the method. The bus number that the WPG was attached to was chosen at random. For all the cases under consideration, the analysis was conducted with and without the optimal placement of the UPFC. In our case, the UPFC has been taken into account for optimal placement in the system, and the relevant data are shown in Table 9. For the maximum scenarios, it is seen that the optimal values of reactance and reactive power injection through the UPFC are same. It indicates the stability of the system with respect to the economy. In this study, the UPFC compensation coefficient was chosen to be between (−0.7) and 0.2, while the range for reactive power injection or extraction was estimated to be between (−100) and 100. These two controlling variables change at regular intervals, and OPF was performed in every case to determine the best outcome. The total system profit has been seen to improve when a wind power source is connected to a bus (shown in Figure 17). Therefore, despite a high initial investment cost, more profit was achieved once the wind power generator was installed.

The changes in bus voltages are depicted in Figure 18. From the graphical representation of the bus voltage data as shown in Figure 18, it is clear that employing the UPFC

enhanced the system’s voltage profile as well. The variation in the LMP value before and after installation of the UPFC for regulated, single-bus deregulated, and double-bus deregulated systems can be seen in Figure 19. From Figure 19, It is obvious that the LMP improved after the UPFC was installed.

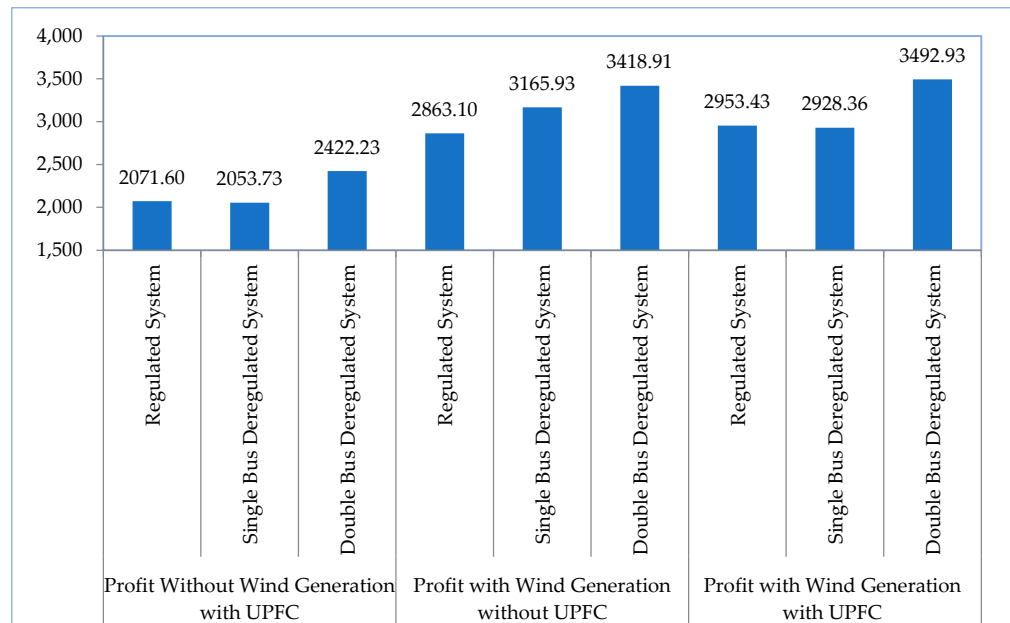


Figure 17. Comparison of system profit for different cases.

Table 9. UPFC optimal location data for different cases.

|  | Regulated without WPG | Regulated with WPG | Single-Bus Deregulated without WPG | Single-Bus Deregulated with WPG | Double-Bus Deregulated without WPG | Double-Bus Deregulated with WPG |
|--|-----------------------|--------------------|------------------------------------|---------------------------------|------------------------------------|---------------------------------|
| UPFC Optimal Location at Line No.              | 5                     | 5                  | 5                                  | 5                               | 9                                  | 5                               |
| UPFC Optimal Location at Bus No.               | 2                     | 2                  | 2                                  | 2                               | 6                                  | 2                               |
| Optimal Value of UPFC (X_range of series side) | -0.25                 | -0.25              | -0.25                              | -0.25                           | 0.2                                | -0.25                           |
| Optimal Value of UPFC (X_range of shunt side)  | -2                    | -2                 | -2                                 | -2                              | -2                                 | -2                              |

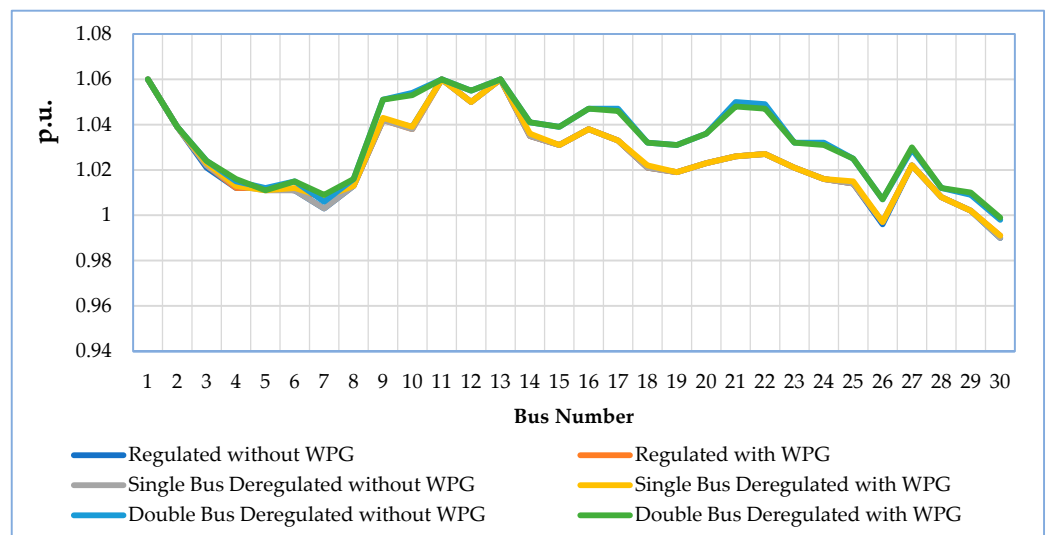
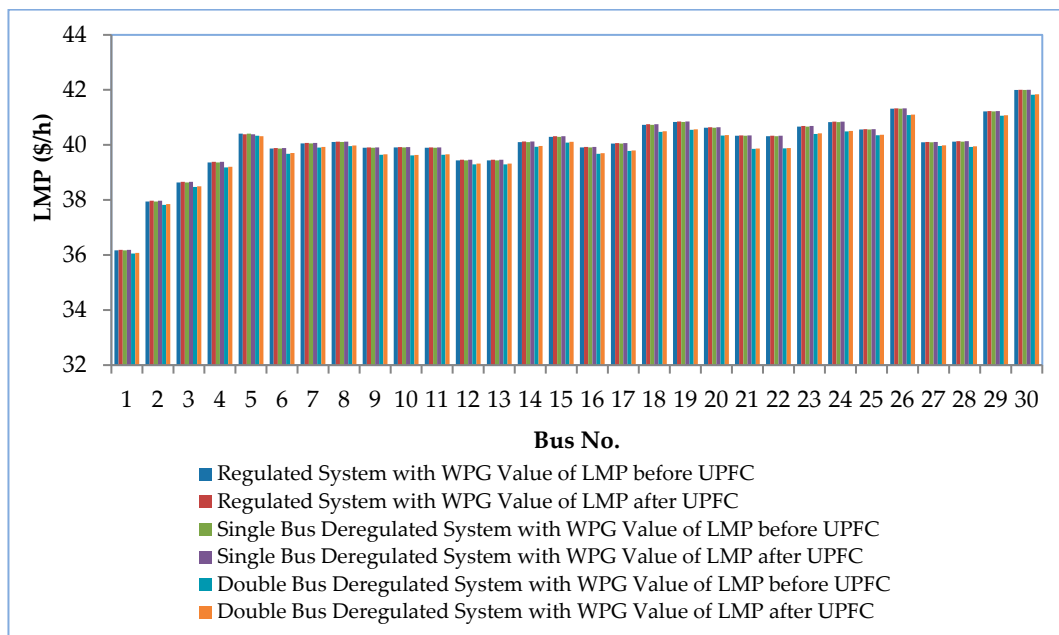


Figure 18. Comparison of bus voltage with a UPFC before and after wind power integration.



**Figure 19.** Variation in LMP at different buses for various cases.

### 5.7. Case 5: System Performance with Wind Farm and Fuel Cell Deployment

This part outlines the system economic assessments of the deregulated wind-integrated power system with the integration of fuel cells. From the preceding section, it is clear that the negative effects of imbalance costs reduce system profit. By installing the fuel cell system, the cost imbalance problem may be resolved. When wind power is available and during off-peak load periods, the fuel cell operates in charging mode. During peak load periods, it operates in discharge mode. Fuel cells can add some extra power to the system during periods of high load and lessen the difference between the planned and actual wind power schedules. In the modified IEEE 30-bus system, a fixed generating capacity with a 4 MW fuel cell system has been installed on bus number 6. The bus for the installation of the fuel cell was chosen using the logic of the greatest number of transmission lines connected to that particular bus.

Different optimization techniques, such as ABC and MFO, have been used alongside SQP to test the capabilities and applicability of the given method. The controlling variables for the MFO and ABC algorithms were taken from references [25,44–47]. The average hourly profits for Mumbai and Delhi using various optimization strategies are shown in Table 10 and Figure 20.

The results indicate that the system profits produced by the addition of fuel cells to the system are larger than those produced by a wind-integrated electrical system without fuel cells. This paper's fundamental novelty is in applying MFO optimization for the first time to an economic problem of this nature. In terms of system profit maximization, MFO outperforms the other two applied optimization algorithms for all consideration circumstances. The placement of the fuel cells and the use of MFO procedures thereby enhance system profits in the context of an unbalanced cost.

**Table 10.** Average hourly profit for Mumbai and Delhi using various optimization strategies.

| Optimization Techniques | Conditions            | Mumbai           |                                   | Delhi            |                                   |
|-------------------------|-----------------------|------------------|-----------------------------------|------------------|-----------------------------------|
|                         |                       | Regulated System | Deregulated System—Double-Bus DSB | Regulated System | Deregulated System—Double-Bus DSB |
| SQP                     | With WF               | 2162.956         | 2588.267                          | 2153.843         | 2528.186                          |
|                         | With WF and Fuel Cell | 2164.625         | 2589.924                          | 2155.538         | 2529.965                          |
|                         | With WF and UPFC      | 2165.538         | 2590.837                          | 2156.429         | 2530.854                          |
| ABC                     | With WF               | 2164.456         | 2589.721                          | 2155.364         | 2529.725                          |
|                         | With WF and Fuel Cell | 2166.358         | 2591.629                          | 2157.219         | 2531.693                          |
|                         | With WF and UPFC      | 2167.235         | 2592.538                          | 2158.129         | 2532.535                          |
| MFO                     | With WF               | 2165.563         | 2590.814                          | 2156.421         | 2530.816                          |
|                         | With WF and Fuel Cell | 2167.683         | 2592.931                          | 2158.563         | 2532.927                          |
|                         | With WF and UPFC      | 2168.529         | 2593.824                          | 2159.428         | 2533.825                          |

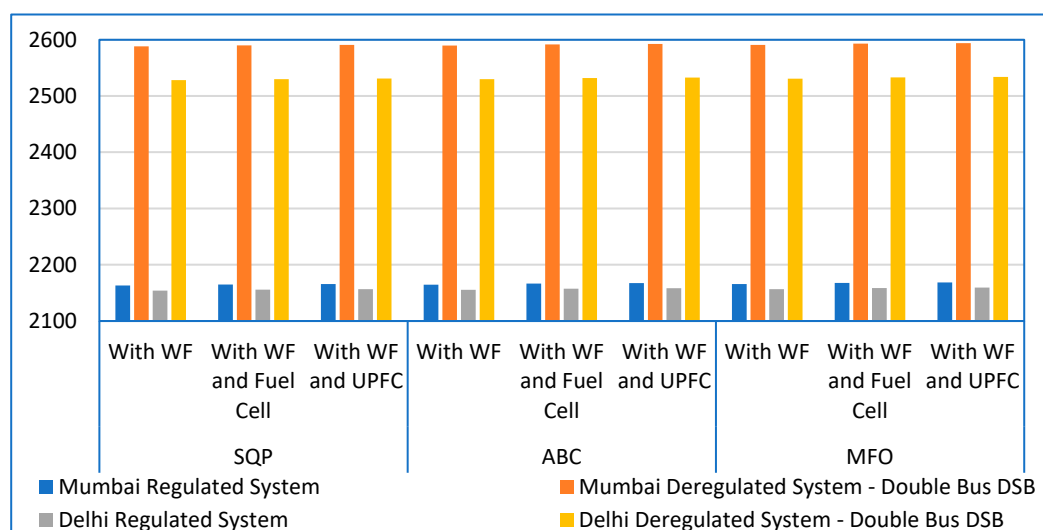


**Figure 20.** Average hourly profit (\$/day) using various optimization methodologies.

*5.8. Case 6: System Risk Analysis Considering the positioning of the Wind Farm, Fuel Cell, and UPFC*

The secure operation of an electrical system largely depends on system risk analysis. In the event that a fault has developed in the system, it must be fixed right away to prevent the failure of the system. The system risk has been determined using the risk analysis tools (VaR and CVaR) based on the LMP of each bus in the system under various scenarios. All of the risk data were determined with a 95% confidence level. The system risk for Delhi is shown in Table 11 and Figure 21 for various system configurations and optimization techniques. The application of MFO algorithms allows for the operation of the most wind farms with the lowest level of system risk. The system risk was decreased once the fuel cell and the UPFC were put into the system. By supplying more electricity locally, the load on the grid was reduced, which is why this occurred.

**Table 11.** System risk for Delhi using multiple optimization techniques and various system situations.

| Sl. No. | Wind Power | VaR               |                           |                           |                           | CVaR              |                           |                           |                           |
|---------|------------|-------------------|---------------------------|---------------------------|---------------------------|-------------------|---------------------------|---------------------------|---------------------------|
|         |            | With WF Using SQP | With WF-FC-UPFC Using SQP | With WF-FC-UPFC Using ABC | With WF-FC-UPFC Using MFO | With WF Using SQP | With WF-FC-UPFC Using SQP | With WF-FC-UPFC Using ABC | With WF-FC-UPFC Using MFO |
| 1       | 10.3 MW    | -0.4205           | -0.4103                   | -0.4023                   | -0.3907                   | -0.5807           | -0.5714                   | -0.5604                   | -0.5504                   |
| 2       | 8.1 MW     | -0.4234           | -0.4122                   | -0.4046                   | -0.3926                   | -0.5851           | -0.5774                   | -0.5662                   | -0.5545                   |
| 3       | 3.42 MW    | -0.424            | -0.4135                   | -0.4057                   | -0.393                    | -0.586            | -0.578                    | -0.5653                   | -0.5556                   |

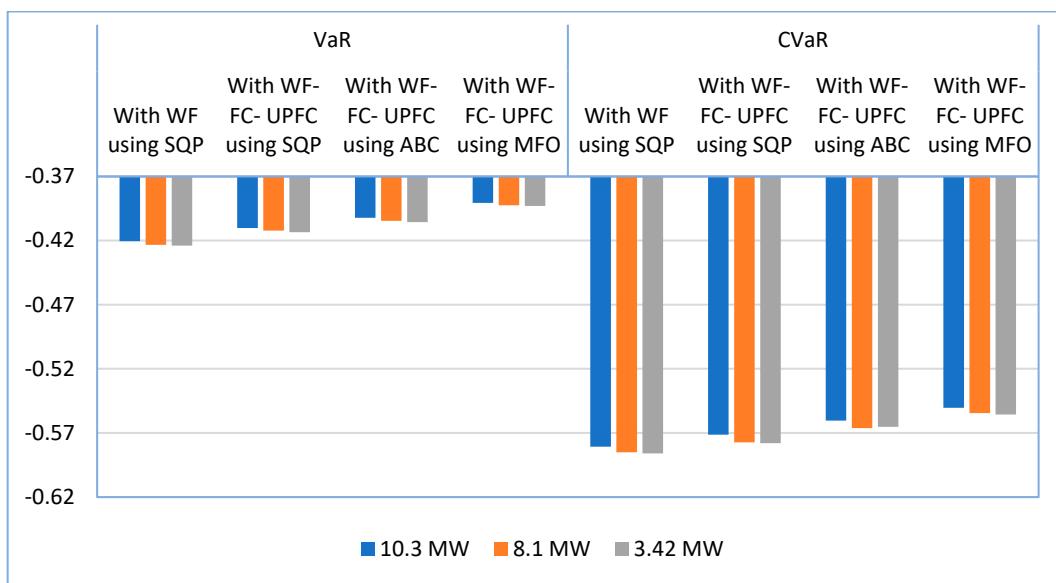


**Figure 21.** System risk with different optimization techniques for Delhi.

### 6. Conclusions

The optimum parameter settings for the UPFC and fuel cells in the regulated and deregulated power systems were presented in this research using different optimization techniques to mitigate the system risk and maximize the economic sustainability of the systems. On modified IEEE 30-bus test systems, the proposed methodology was performed. The test results demonstrated the viability of the suggested strategy. The goal of this study was to maximize societal welfare and system profit while minimizing the objective function using the cost models of UPFCs, fuel cells, and wind power generation. It has been noted that:

- (a) After adding the wind generator to the system, a UPFC was employed to mitigate the issues;
- (b) Fuel cells were successful in improving social welfare and cost imbalances;
- (c) SW became better once a UPFC was included to the pool model;
- (d) By integrating the UPFC and fuel cells with the WPG, the locational marginal price of the system significantly decreased;
- (e) The voltage profile in UPFC operation with the WPG was also stable.

This proposed approach is a universal method that may be utilized to enhance any size, type, integrated, or deregulated electrical system. In the future, this work can be performed with different renewable energy sources along with different optimization techniques to enhance system security and stability.

**Author Contributions:** Conceptualization, M.R.C. and S.D.; methodology, M.R.C., S.D. and J.B.B.; software, M.R.C.; validation, P.K.S. and T.S.U.; formal analysis, S.D. and T.S.U.; investigation, M.R.C., J.B.B. and T.S.U.; resources, M.R.C. and S.D.; data curation, P.K.S.; writing—original draft preparation, M.R.C. and J.B.B.; writing—review and editing, S.D., P.K.S. and T.S.U.; visualization, S.D.; supervision,

P.K.S. and T.S.U.; project administration, T.S.U.; funding acquisition, T.S.U. All authors have read and agreed to the published version of the manuscript.

**Funding:** This research received no external funding.

**Institutional Review Board Statement:** Not applicable.

**Informed Consent Statement:** Not applicable.

**Data Availability Statement:** Not applicable.

**Conflicts of Interest:** The authors declare no conflict of interest.

## Abbreviations

|  |  |
|--|--|
| $WS_h$   | wind speed (at any height 'h')   |
| $WS_r$   | reference wind speed (at a height of 10 m')  |
| $N$  | Hellman's coefficient  |
| $D_{air}$                                      | air density (in $kg/m^3$ )   |
| $A_t$  | turbine's swept area (in $m^2$ ),  |
| $\eta$   | efficiency (overall) of the wind plant   |
| $X_{upfc}$                                     | UPFC's series converter's reactance  |
| $IC_{upfc}$                                    | UPFC's investment cost   |
| $E_{elz}$                                      | energy consumed by the electrolyzer  |
| $\eta_{elz}$                                   | efficiency of the electrolyzer   |
| $E_{fc}$                                       | energy produced from the fuel cell   |
| $\eta_{fc}$                                    | efficiency of the fuel cell  |
| $C(i)_{PG(i)}$                                 | apparent cost of production  |
| $B(j)_{PD(j)}$                                 | consumer benefit   |
| $P_{n(t)}$                                     | the n-th unit's total profit at a time 't'   |
| $TR_{n(t)}$                                    | total revenue  |
| $IMC_{n(t)}$                                   | total imbalance cost   |
| $TGC_{n(t)}$                                   | overall generation cost  |
| $P_{a,i(t)}$                                   | power generated with actual wind speed at a time 't' at the i-th generation bus                      |
| $P_{f,i(t)}$                                   | power generated with forecasted wind speed   |
| $CR_s(t)$                                      | charge rate (surplus)  |
| $CR_d(t)$                                      | charge rate (deficit).   |
| $LMP_i(t)$                                     | LMP at time 't' at the i-th bus  |
| $GC_m(t)$                                      | power generation cost of the thermal unit  |
| $N_{upfc}$                                     | the total number of UPFC devices   |
| $N_{wind}$                                     | the total number of linked wind generators   |
| $P_{G,i}$                                      | generated power at the i-th generation unit  |
| $P_w$  | wind power   |
| $P_L$  | line loss  |
| $P_D$  | power demand   |
| $N_L$  | No. of transmission lines  |
| $G_{i-j}$                                      | line conductance of line between bus 'i' and 'j'   |
| $\delta_i,  V_i $                              | phase angle and voltage magnitude of bus 'i'   |
| $\delta_j,  V_j $                              | phase angle and voltage magnitude of bus 'j'   |
| $P_i$  | real power injected at the bus 'i'   |
| $Q_i$  | reactive power injected at the bus 'i'   |
| $\theta_{ik}, Y_{ik}$                          | angle and magnitude of the element of the i-th row and the k-th column of the bus admittance matrix. |
| $V_{i(\min)}, V_{i(\max)}$                     | lower and upper voltage limit of bus 'i'   |
| $\varnothing_{i(\min)}, \varnothing_{i(\max)}$ | lower an upper angle limit corresponding to the voltage of bus 'i'                                   |
| $LF_l, LF_{l(\max)}$                           | actual and maximum line flow of line 'l'   |
| $PG_{i(\min)}, PG_{i(\max)}$                   | lower and upper real power limit of bus 'i'  |
| $QG_{i(\min)}, QG_{i(\max)}$                   | lower and upper reactive power limit of bus 'i'  |

## References

1. Odara, S.; Khan, Z.; Ustun, T.S. Optimizing energy use of SmartFarms with smartgrid integration. In *2015 3rd International Renewable and Sustainable Energy Conference (IRSEC)*; IEEE: Piscatavie, NJ, USA, 2015; pp. 1–6.
2. Regy, P.V.; Sarwal, R.; Stranger, C.; Fitzgerald, G.; Ningthoujam, J.; Gupta, A.; Singh, N. *Turning Around the Power Distribution Sector: Learnings and Best Practices from Reforms*; NITI Aayog, RMI, and RMI India: New Delhi, India, 2021; ISBN 978-81-949510-3-2. [CrossRef]
3. Owusu, P.A.; Asumadu-Sarkodie, S. A review of renewable energy sources, sustainability issues and climate change mitigation. *Cogent Eng.* **2016**, *3*, 1167990. [CrossRef]
4. Adetokun, B.B.; Muriithi, C.M. Application and control of flexible alternating current transmission system devices for voltage stability enhancement of renewable-integrated power grid: A comprehensive review. *Heliyon* **2021**, *7*, e06461. [CrossRef] [PubMed]
5. Ma, Z.; Josh, E.; Jennifer, K. Fuel Cell Backup Power System for Grid Service and Micro-Grid in Telecommunication Applications: Preprint. National Renewable Energy Laboratory: Golden, CO, USA, 2018; NREL/CP-5500-70990. Available online: <https://www.nrel.gov/docs/fy18osti/70990.pdf> (accessed on 5 October 2022).
6. Cui, J.; Li, Y.; He, C.; Zhang, Z.; Wang, H.; Tang, J.; Li, Y.; Cai, H.; Lin, Z.; Yang, L. Optimal Electricity Allocation Model Under China's Planning-Market Double-Track Mechanism Considering Bidding Game of Generation Companies. *Front. Energy Res.* **2021**, *9*, 673228. [CrossRef]
7. Ugurlu, U.; Tas, O.; Kaya, A.; Oksuz, I. The Financial Effect of the Electricity Price Forecasts' Inaccuracy on a Hydro-Based Generation Company. *Energies* **2018**, *11*, 2093. [CrossRef] [PubMed]
8. Conejo, A.J.; Nogales, F.J.; Arroyo, J.M. Price-taker bidding strategy under price uncertainty. *IEEE Trans. Power Syst.* **2002**, *17*, 1081–1088. [CrossRef]
9. Basu, J.B.; Dawn, S.; Saha, P.K.; Chakraborty, M.R.; Ustun, T.S. A Comparative Study on System Profit Maximization of a Renewable Combined Deregulated Power System. *Electronics* **2022**, *11*, 2857. [CrossRef]
10. Selvaraju, R.K.; Somaskandan, G. Impact of energy storage units on load frequency control of deregulated power systems. *Energy* **2016**, *97*, 214–228. [CrossRef]
11. Zhu, X.; Dichen, L.; Wu, J. Two-Stage Optimal Location Allocations of DPFC Considering Wind and Load Uncertainty. *Front. Energy Res.* **2022**, *10*, 865902. [CrossRef]
12. Pandian, M.S.; Makbul, A.; Husodo, B.Y.; Ayong, H. Efficiency and economics analysis of Proton Exchange Membrane fuel cell. In *Proceedings of the 2010 Conference Proceedings IPEC, Singapore, 27–29 October 2010*; pp. 875–880. [CrossRef]
13. Available online: <https://electrek.co/2022/08/24/fuel-cells-solar-wind/> (accessed on 10 October 2022).
14. Singh, N.K.; Koley, C.; Gope, S.; Dawn, S.; Ustun, T.S. An Economic Risk Analysis in Wind and Pumped Hydro Energy Storage Integrated Power System Using Meta-Heuristic Algorithm. *Sustainability* **2021**, *13*, 13542. [CrossRef]
15. Albogamy, F.R.; Khan, S.A.; Hafeez, G.; Murawwat, S.; Khan, S.; Haider, S.I.; Basit, A.; Thoben, K.-D. Real-Time Energy Management and Load Scheduling with Renewable Energy Integration in Smart Grid. *Sustainability* **2022**, *14*, 1792. [CrossRef]
16. Fathy, A.; Alharbi, A.G. Recent approach based movable damped wave algorithm for designing fractional-order PID load frequency control installed in multi-interconnected plants with renewable energy. *IEEE Access* **2021**, *9*, 71072–71089. [CrossRef]
17. Elshahed, M.; Tolba, M.A.; El-Rifaie, A.M.; Ginidi, A.; Shaheen, A.; Mohamed, S.A. An Artificial Rabbits' Optimization to Allocate PVSTATCOM for Ancillary Service Provision in Distribution Systems. *Mathematics* **2023**, *11*, 339. [CrossRef]
18. Shaheen, A.M.; Elsayed, A.M.; El-Sehiemy, R.A.; Kamel, S.; Ghoneim, S.S.M. A modified marine predators optimization algorithm for simultaneous network reconfiguration and distributed generator allocation in distribution systems under different loading conditions. *Eng. Optim.* **2021**, *54*, 687–708. [CrossRef]
19. Dey, P.P.; Das, D.C.; Latif, A.; Hussain, S.M.S.; Ustun, T.S. Active Power Management of Virtual Power Plant under Penetration of Central Receiver Solar Thermal-Wind Using Butterfly Optimization Technique. *Sustainability* **2020**, *12*, 6979. [CrossRef]
20. Chauhan, A.; Upadhyay, S.; Khan, M.T.; Hussain, S.M.S.; Ustun, T.S. Performance Investigation of a Solar Photovoltaic/Diesel Generator Based Hybrid System with Cycle Charging Strategy Using BBO Algorithm. *Sustainability* **2021**, *13*, 8048. [CrossRef]
21. Hussain, I.; Das, D.C.; Sinha, N.; Latif, A.; Hussain, S.M.S.; Ustun, T.S. Performance Assessment of an Islanded Hybrid Power System with Different Storage Combinations Using an FPA-Tuned Two-Degree-of-Freedom (2DOF) Controller. *Energies* **2020**, *13*, 5610. [CrossRef]
22. India Meteorological Department, Ministry of Earth Sciences, Government of India. AWS Lab, Pune. Available online: <http://www.imd.gov.in/Welcme%20To%20IMD/Welcme.phpandhttp://www.imdaws.com/ViewAwsData.aspx> (accessed on 13 November 2022).
23. Database: World Temperatures-Weather around the World. Available online: [www.timeanddate.com/weather](http://www.timeanddate.com/weather) (accessed on 15 November 2022).
24. Dawn, S.; Tiwari, P.K.; Goswami, A.K. An approach for efficient assessment of the performance of double auction competitive power market under variable imbalance cost due to high uncertain wind penetration. *Renew. Energy* **2017**, *108*, 230–243. [CrossRef]
25. Morthorst, P.E. *Wind Energy—The Facts: Costs & Prices*; RISO National Laboratory: Roskilde, Denmark, 2010; Volume 2, pp. 94–110.
26. Gerbex, S.; Cherkaoui, R.; Germond, A.J. Optimal location of multi-type FACTS devices in a power system by means of genetic algorithms. *IEEE Trans. Power Syst.* **2001**, *16*, 537–544. [CrossRef]

27. Lie, T.T.; Deng, W. Optimal flexible AC transmission systems (FACTS) devices allocation. *Int. J. Electr. Power Energy Syst.* **1997**, *19*, 125–134. [[CrossRef](#)]
28. Zahid, M.; Chen, J.; Li, Y.; Duan, X.; Lei, Q.; Bo, W.; Mohy-ud-din, G.; Waqar, A. New Approach for Optimal Location and Parameters Setting of UPFC for Enhancing Power Systems Stability under Contingency Analysis. *Energies* **2017**, *10*, 1738. [[CrossRef](#)]
29. Tiwari, P.K.; Sood, Y.R. An Efficient Approach for Optimal Allocation and Parameters Determination of TCSC with Investment Cost Recovery under Competitive Power Market. *IEEE Trans. Power Syst.* **2013**, *28*, 2475–2484. [[CrossRef](#)]
30. Tiwari, P.K.; Sood, Y.R. Efficient and optimal approach for location and parameter setting of multiple unified power flow controllers for a deregulated power sector. *IET Gener. Transm. Distrib.* **2012**, *6*, 958–967. [[CrossRef](#)]
31. Mithulanathan, N.; Acharya, N. A proposal for investment recovery of FACTS devices in deregulated electricity markets. *Electr. Power Syst. Res.* **2007**, *77*, 695–703. [[CrossRef](#)]
32. Wibowo, R.S.; Yorino, N.; Eghbal, M.; Zoka, Y.; Sasaki, Y. FACTS devices allocation with control coordination considering congestion relief and voltage stability. *IEEE Trans. Power Syst.* **2011**, *26*, 2302–2310. [[CrossRef](#)]
33. Saravanan, M.; Slochanal, S.M.R.; Venkatesh, P.; Abraham, J.P.S. Application of particle swarm optimization technique for optimal location of FACTS devices considering cost of installation and system loadability. *Electr. Power Syst. Res.* **2007**, *77*, 276–283. [[CrossRef](#)]
34. Habur, K.; O’Leary, D. FACTS for Cost Effective and Reliable Transmission of Electrical Energy. Available online: [www.worldbank.org/html/fpd/em/transmission/facts\\_siemens.pdf](http://www.worldbank.org/html/fpd/em/transmission/facts_siemens.pdf) (accessed on 12 October 2022).
35. Lashkar Ara, A.; Kazemi, A.; Nabavi Niaki, S.A. Multiobjective optimal location of FACTS shunt-series controllers for power system operation planning. *IEEE Trans. Power Deliv.* **2011**, *27*, 481–490. [[CrossRef](#)]
36. Ural Bayrak, Z.; Gençoğlu, M.T. Mathematical Models of PEM Fuel Cells. In Proceedings of the 5th International Ege Energy Symposium and Exhibition (IEESE-5), Denizli, Turkey, 27–30 June 2010.
37. Shrestha, G.B.; Fonseka, P.A.J. Congestion-driven transmission expansion in competitive power markets. *IEEE Trans. Power Syst.* **2004**, *19*, 1658–1665. [[CrossRef](#)]
38. Dawn, S.; Tiwari, P.K. Improvement of economic profit by optimal allocation of TCSC & UPFC with wind power generators in double auction competitive power market. *Int. J. Electr. Power Energy Syst.* **2016**, *80*, 190–201. [[CrossRef](#)]
39. Das, A.; Dawn, S.; Gope, S.; Ustun, T.S. A Strategy for System Risk Mitigation Using FACTS Devices in a Wind Incorporated Competitive Power System. *Sustainability* **2022**, *14*, 8069. [[CrossRef](#)]
40. Omran, A.; Lucchesi, A.; Smith, D.; Alaswad, A.; Amiri, A.; Wilberforce, T.; Sodré, J.R.; Olabi, A.G. Mathematical model of a proton-exchange membrane (PEM) fuel cell. *Int. J. Thermofluids* **2021**, *11*, 100110. [[CrossRef](#)]
41. Dufo-Lopez, R.; Bernal-Agustín, J.L.; Contreras, J. Contreras Javier, Optimization of control strategies for stand-alone renewable energy systems with hydrogen storage. *Renew. Energy* **2007**, *32*, 1102–1126. [[CrossRef](#)]
42. Mahdad, B.; Srairi, K.; Bouktir, T. Optimal power flow for large-scale power system with shunt FACTS using efficient parallel GA. *Electr. Power Energy Syst.* **2012**, *32*, 507–517. [[CrossRef](#)]
43. Zimmerman, R.D.; Murillo-Sanchez, C.E.; Gam, D. MATPOWER—A MATLAB Power System Simulation Package, Version 3. Available online: <https://www.pserc.cornell.edu/matpower> (accessed on 3 October 2022).
44. Das, A.; Dawn, S.; Gope, S.; Ustun, T.S. A Risk Curtailment Strategy for Solar PV-Battery Integrated Competitive Power System. *Electronics* **2022**, *11*, 1251. [[CrossRef](#)]
45. Idir, A.; Canale, L.; Bensafia, Y.; Khettab, K. Design and Robust Performance Analysis of Low-Order Approximation of Fractional PID Controller Based on an IABC Algorithm for an Automatic Voltage Regulator System. *Energies* **2022**, *15*, 8973. [[CrossRef](#)]
46. Fathy, A.; Kassem, A.; Zaki, Z.A. A Robust Artificial Bee Colony-Based Load Frequency Control for Hydro-Thermal Interconnected Power System. *Sustainability* **2022**, *14*, 13569. [[CrossRef](#)]
47. Rezk, H.; Zaky, M.M.; Alhaider, M.; Tolba, M.A. Robust Fractional MPPT-Based Moth-Flame Optimization Algorithm for Thermoelectric Generation Applications. *Energies* **2022**, *15*, 8836. [[CrossRef](#)]

**Disclaimer/Publisher’s Note:** The statements, opinions and data contained in all publications are solely those of the individual author(s) and contributor(s) and not of MDPI and/or the editor(s). MDPI and/or the editor(s) disclaim responsibility for any injury to people or property resulting from any ideas, methods, instructions or products referred to in the content.